Invited Review Paper

Present Status and Future Prospect of Widegap Semiconductor High-Power Devices

Hajime OKUMURA*

*Power Electronics Research Center, National Institute of Advanced Industrial Science and Technology,
Central 2, 1-1-1 Umezono, Tsukuba, Ibaraki 305-8568, Japan*

High-power device technology is a key technological factor for wireless communication, which is one of the information network infrastructures in the 21st century, as well as power electronics innovation, which contributes considerably to solving the energy saving problem in the future energy network. Widegap semiconductors, such as SiC and GaN, are strongly expected as high-power high-frequency devices and high-power switching devices owing to their material properties. In this paper, the present status and future prospect of these widegap semiconductor high-power devices are reviewed, in the context of applications in wireless communication and power electronics. [DOI: 10.1143/JJAP.45.7565]

1. Introduction

For information and communication technology and electric power control technology needed to support modern human society, electronics is the basic technological domain that we cannot lack in. Si, GaAs, and their related materials are currently used widely in electronics. The constituting elements of these semiconductor materials are mainly located below the third period in the periodic table. On the other hand, SiC and GaN, which include the elements on the second period in the periodic table such as N and C, have gradually attracted much attention under the concept of "Hard Electronics",[1] in several electronics application fields that cannot be covered by these conventional semiconductor materials. A semiconductor including elements on the second period is a widegap semiconductor having the characteristics of smaller lattice constants and larger bandgap energy than those of Si and GaAs. A small lattice constant necessarily leads to a strong atomic bond, and several characteristic parameters of widegap semiconductors, such as thermal conductivity, saturation drift velocity, breakdown electric field, have extremely large values due to this strong binding energy. A large bandgap energy, which means that the absorbed or emitted light has a short wavelength, is also caused by the small atomic distance in crystal.

Nowadays, several application fields where the use of conventional electronics became essentially difficult have been revealed as a result of the expansion of electronics to various kinds of application, because the characteristic parameters of Si and GaAs are not enough as semiconductor materials. These fields include low-loss switching devices which are important components of high-power high-efficiency inverters in the future novel power electronics system, and high-power high-frequency (HF) devices which are the key devices of wireless communication infrastructure, such as next-generation mobile telephones, satellite communications, and fixed wireless access in the future information and communication network society. In these technological domains, any essential development cannot be expected even though there are huge needs, as long as Si or GaAs is used as a semiconductor material for electronics.

For a breakthrough in these domains, the development of high-performance devices made of widegap semiconductors such as SiC and GaN is indispensable. In fact, the innovation has come to exhibit a reality owing to the recent progress of device process and crystal growth technologies for these widegap semiconductors.[2,3]

It is well known that short wavelength optical devices made of GaN-related materials have appeared in the market in the past several years. Also, the research and development of high-power, high-frequency, low-loss, and high-efficiency electron devices made of III–nitrides and SiC have made markedly rapid progress. These materials are key technologies for future information and communication systems and power electronics network systems. In this review, the present status of widegap semiconductor high-power electron devices is examined, and their future prospect is discussed.

2. Infrastructure Requirements for High-Power Devices

2.1 Wireless communication

For the development of information and communication technology to support the advanced information society of the 21st century, the large-capacity high-speed information communication connecting a wide range of information processing hardware to a network is indispensable, in addition to the information processing based on Si ultra-large-scale integrated circuits. It is wireless communication technology that is expected as a leading technology for superhigh-speed communication networks, together with optical communication technology. Concerning the access system, which is complementary with the communication backbone system, it is certain that wireless communication will become the mainstream considering the recent technology trend, portability, convenience such as the nonrequirement of wiring, and the extent of the application area in the near future. In fact, one hundred and several tens of Mbps class speed will be required for a mobile access system, and a high-power HF device operating with high efficiency in the frequency range from several GHz to several tens of GHz is the most important key issue for this purpose.

2.1.1 Various wireless communication systems

Wireless communication technology is divided into

*E-mail address: h-okumura@aist.go.jp
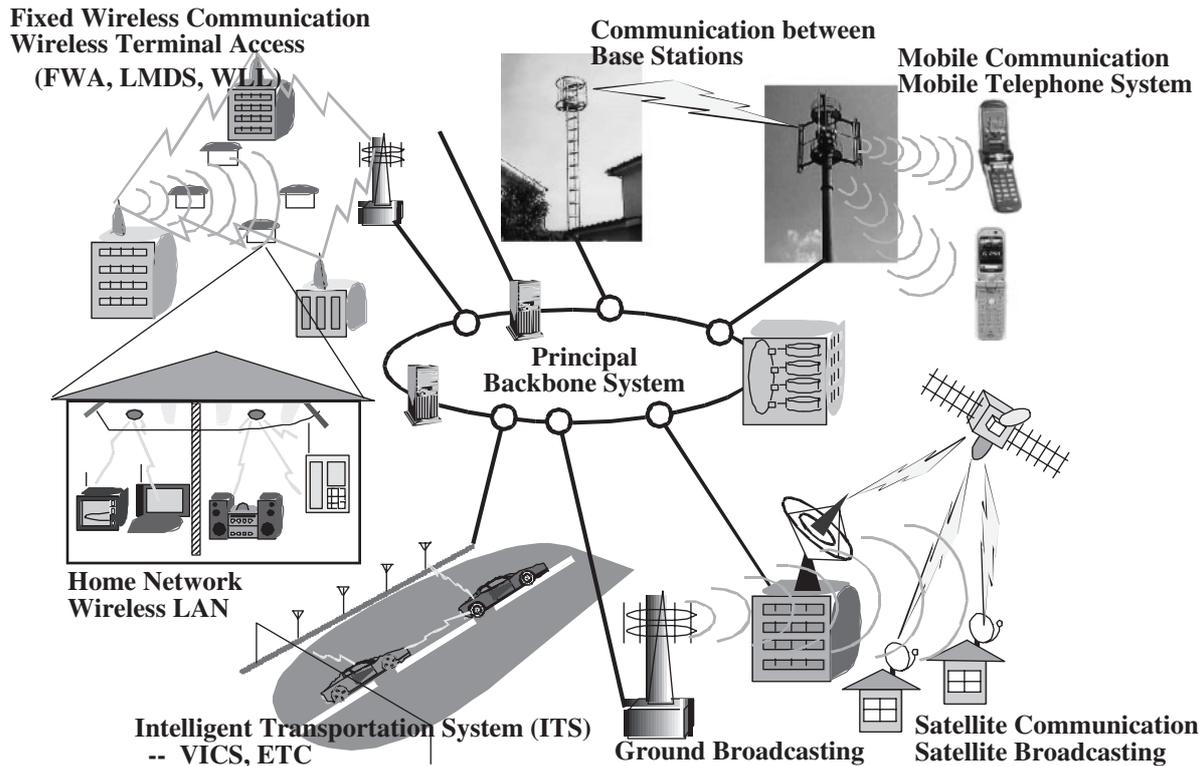
Fig. 1.   Various kinds of wireless communication systems. FWA: fixed wireless access, LMDS: local multipoint distribution system, WLL: wireless local loop, ITS: intelligent transportation system, VICS: vehicle information communication system, ETC: electronic toll collection.

mobile communication, fixed communication, satellite communications, home networks, broadcasting, remote sensing and other fields from the viewpoint of use (cf. Fig. 1). Because the utilization style of electromagnetic waves and demanded communication quality are different, the frequency used, necessary electric power, communication distance, and modulation method differ from one another.

In these several years, mobile communication is the field where its utilization has made an explosive expansion, as represented by mobile telephones. From the point of an antenna size that can secure portability and sufficient communication distance with minimized attenuation, ultrahigh frequency [UHF (30–300 MHz)] and very high frequency [VHF (300 MHz–3 GHz)] bands have been used for exterior use by analog modulation. In recent mobile telephone systems, the frequency used has shifted to the L-band (1–2 GHz band) compared with the conventional outdoor analog communication from the viewpoint of high speed and broad bandwidth by digital modulation. By International Mobile Telecommunications 2000 (IMT-2000), whose service started in 2001 with the 2.2 GHz band, high-speed digital communication at rates of 64–144 kbps during high-speed movement, 64–384 kbps for walking speed and as high as 2 Mbps for indoor use are respectively possible, and it enables even the transmission of an animation. In the future, fusion with the Internet will make more progress from the user side, and it seems that the telephone exchange network system for mobile communication will also shift to an Internet-based one.

In the field of fixed communication, the microwave band of 4–11 GHz has been mainly used for long-distance communication out of the necessity of large-capacity transmission. In this system, high-multiplicity digital modulation is adopted, and a transmission speed as high as 300 Mbps per frequency is enabled. In recent years, the necessity of large-capacity digital communication to office buildings and for home use has been revealed with the development of the Internet, and progress in this field is expected as a fixed wireless access (FWA) system, which is called a local multipoint distribution system (LMDS) or a wireless local loop (WLL) and oriented to short-distance large-capacity fixed communication within approximately several km. In this application, 22/26/38 GHz bands are used to make a broader bandwidth possible, and a transmission speed of approximately 100 Mbps for point-to-point or 10 Mbps for point-to-multipoints is assumed.

Satellite communications have been widely used in various mobile and fixed communication networks and broadcasting. For transmitters and devices used in this field, a high-power characteristic is critical from the viewpoint of transmission distance, compared with other ground communications. High-efficiency, high-reliability, long-lifetime characteristics are also critical from the requirement of cost. It is expected that this technological field will be used in the installation of a large-scale relay station on a geostationary orbit or in the stratosphere, or a low-orbit satellite in the future.

With the spread of the Internet, demand for broadband Internet access from offices and homes has occurred. The FWA mentioned above aims at the expansion of broadband service to offices and homes through a wireless access system. The trend in which the corresponding wiring in

offices/homes is shifting to being wireless is now remarkable. The development of a wireless network to connect household electric appliances is also in progress, besides the use of a wireless LAN with the 2.4 or 5.2 GHz band.

Furthermore, wireless communication technology also plays an important role in intelligent transportation system (ITS), in the form of remote sensing technology. Electronic toll collection (ETC) for bill receipt system and vehicle information communication system (VICS) for vehicle information transmission are now at the stage of practical use. For communication and distance-measuring radar between a path and a car and between cars, a trial of systematization using the millimeterwave region of 60/80 or 5.8 GHz is in progress. As an individual in-vehicle system, there are applications to short-distance radar for garaging and collision prevention. In USA, the development of a radar system for military use using the 10 GHz band is becoming a major objective.

I try to consider HF devices used for various systems from the viewpoint of output power. Devices of low power less than several W are used for terminals of so-called mobile communication systems, such as personal handyphone systems (PHSs), mobile telephones, mobile PCs. The present commercial frequencies are in the microwave region from several 100 MHz to several GHz; however, the shift to higher frequency is inevitable because of the increase in information traffic and the enlarged demand for frequency resources. On the other hand, devices of intermediate-level power from several 10 W to several 100 W are used for base stations of mobile communication and FWA, whose future development is greatly anticipated. Higher power devices than the above are used in communication satellites and various broadcasting networks. For these communication infrastructures, the high output power of a device is strongly demanded by various kinds of requests, as will be described later. Furthermore, there is also an application to radar systems by pulsed operation using ultrahigh power.

2.1.2 Performance required for HF device for wireless communication systems

Wireless communication systems have recently shown outstanding progress as demonstrated by a typical example of a mobile telephone system using the L-band. They have progressed throughout towards higher frequencies since the invention of wireless telegraphy by Marconi. The use of several to one hundred and several 10 GHz is expected to be the basis of the wireless digital communication infrastructure for the future information and communication society. Its modulation method has shifted from an analog to a digital one; the latter can make better use of frequency and enables more reliable information transmission. Furthermore, it is evolving to become a novel ultrawide-band (UWB) method, which will change the concept of multiple-value modulation, or a carrier wave and modulation. High-performance HF device technology enabled the development of these wireless communication systems. At present, GaAs devices are mainly used for practical systems in this field. Various novel applications, that were considered impossible before, are expected to develop newly, in accordance with the progress of technological development in the future.

This trend towards high frequency is propelled from the

carrier frequency increase in response to not only a technical request for large capacity and high speed, but also a legal request from the expansion of available frequencies for wireless communication systems, where the frequency bands used are regulated by law. In wireless communication, high output power is essential to secure communication reliability using a higher frequency at the same distance, because the transmission distance of a carrier wave decreases and circuit losses increase with increasing its frequency. On the other hand, the average transmission output power per channel rather tends to decrease owing to the decrease in necessary transmission distance brought about by the introduction of microcell systems and digital modulation. However, current digital communication methods adopt a multicarrier common amplification method, where signals of several communication channels are amplified together. An increase in the number of channels means not only an expansion in bandwidth but also an increase in the total electric power or peak value of the signal that the same output amplifier treats. Thus, a high-output-power amplifier or device becomes necessary accordingly.

Second, the linearity of an amplifier is extremely important (cf. Fig. 2) to avoid interference with an adjacent channel, and the linear region in the input versus output relation of an amplifier device where input/output power is lowered from the saturation region is used in an actual operation. This lowered amount of the power is called back-off, and it is normally set 7–8 dB below (one fifth or sixth) the saturation point of a device. Frequency shift keying (FSK) method and phase shift keying (PSK) method are used, when the digital modulation method of the present wireless communication system is roughly classified. The demand for the linearity of an amplifier and an output circuit is particularly severe for PSK, which enables highly efficient frequency use and is the mainstream of present practical systems. In this sense, the maximum power must be sufficiently higher than the actually used average power, and a considerably high output specification is required for a HF device used for an amplifier. For a base station of IMT-2000, a next-generation mobile telephone system, an output power specification of 500–1000 W per antenna sector is required. In this way, with high-frequency, broad-bandwidth, and high-output-power characteristics, a wireless communication system is requested as the solution for coping with the anticipated explosive information traffic increase in the future, and the expectation for widegap semiconductor devices that can enable the solution is growing. It is anticipated that the output power reaches a limit even with a multitip configuration using GaAs devices, and novel devices such as GaN heterojunction field effect transistors (HFETs) are eagerly desired.

On the other hand, other characteristics are also required for HF devices used in amplifiers, from the viewpoint of energy and resource saving in a wireless communication system, particularly a mobile telephone network system. The efficiency of HF devices used in present mobile base stations is considered to be 30–40%; most of the power loss is through heat generation. In addition, the base stations are equipped with a cooling system for heat dissipation to protect them from the heat. Because of historical circumstances, direct current 48 V, which is the same as the value
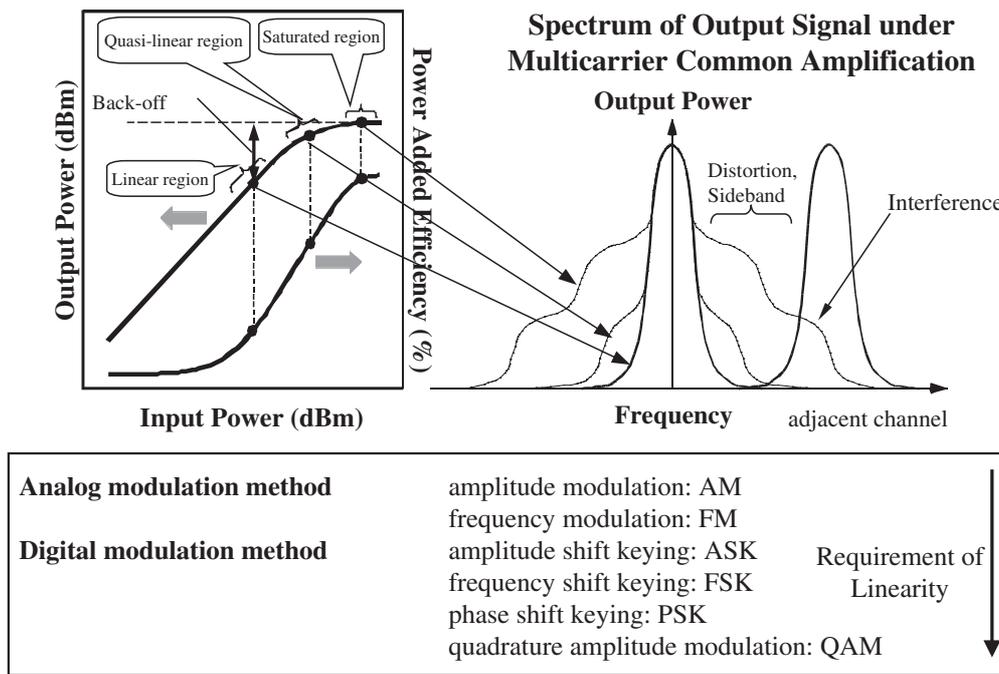
Fig. 2.   Input-output characteristics of HF amplifier used for wireless communication system, and its modulation method.

used in a fixed telephone system, is used for the power supply in a base station. This voltage must be converted into 10–20 V levels with a transformation apparatus for the operation of a HF device in an amplifier. A considerable electric power loss occurs in this voltage conversion. An actual base station using Si and GaAs devices must be equipped with these facilities, and the plant and equipment investment and energy loss for this purpose are enormous. HF devices with 48 V operation and high amplification efficiency, if available, will contribute considerably to energy and resource saving. In addition, the installation of a base station becomes easier with the miniaturization of the system, and the establishment of wireless communication system infrastructure will be greatly promoted. There is a large expectation for widegap semiconductor HF devices that can operate at high voltage from this point of view.

The requests for network devices used for wireless communication are summarized as follows.

1. Higher operation frequency, which enables the expansion of frequency resources, large-capacity high-speed communication, and broad bandwidth.
2. Higher output power, which enables long-distance transmission, broad bandwidth, and low distortion.
3. Higher operation voltage, which enables high efficiency, low energy loss and size reduction.

Monolithic microwave ICs (MMICs) are also effective for the high-speed operation and size reduction of a device. In addition, if the high output operation for one chip is enabled by an MMIC, the mixing loss of output power in a parallel configuration is avoided, and the design of power mixing circuit, which depends considerably on frequency, becomes unnecessary. The versatility of a single HF transistor is greatly increased.

2.2   Power electronics

Besides the information network, our human society depends considerably on another important network, namely, the energy network. All the activities in our modern society have been realized only by consuming various kinds of energy, such as fossil fuel, atomic energy, and solar energy. Several aspects of energy management, i.e., generation, storage, transportation, conversion, and consumption, are highly integrated to form networks on various scales, and these networks much contribute to the activity of human society. It can be said that even the information network and the distribution network for commodities cannot work with the absence of the energy network. The present modes of utilizing energy are generally classified into electricity, heat, chemicals, and other forms. Among these, electricity is the mainstream of the energy network, owing to its ease of management and the variety of available fields. The percentage of energy consumed in the form of electricity is more than 40% in advanced countries, and expected to increase more in the future, in addition to the total energy consumption increase. In this sense, the efficient and reliable management of the electrical energy network and its technological development will be the critical issue for the future sustainable development of human society. Considering the urgent request for the environment to reduce CO_2 emission, the importance of efficient management of the energy network will steadily increase in the future.

Under such a situation, electronics can be also used for electric power management. Power electronics is a technological domain that deals with electric power conversion by switching, which plays an important role in the management and control of the electric energy network. In various energy network systems, quite a large number of power conversions are required for convenient utilization of electric power. Every conversion process inevitably generates a certain amount of energy loss. In this sense, the reduction of energy loss during the conversion is essential in improving the efficiency of the energy network system. Furthermore, the

Jpn. J. Appl. Phys., Vol. 45, No. 10A (2006)

H. OKUMURA
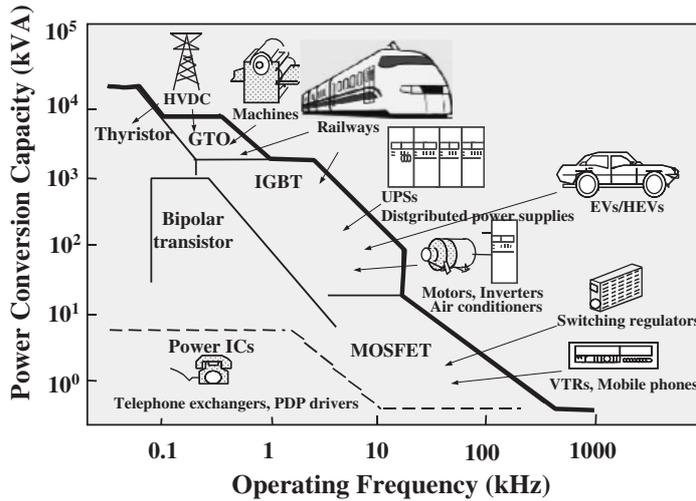
Fig. 3. Various application areas of power electronics, where high-efficiency switching devices are used.

miniaturization of conversion apparatus is also important. For these 40 years, power electronics has developed on the basis of Si devices such as the metal–oxide–semiconductor field effect transistor (MOSFET), gate turn-off thyristor (GTO) and insulated gate bipolar transistor (IGBT); however, the essential limit of these Si devices has been revealed. The expectation for small and low-loss switching devices based on widegap semiconductors has recently increased, owing to their superior material properties. This situation is quite similar to that of HF devices.

2.2.1 Various power electronics system

It is rare that generated electric power is directly used. In most cases, various features of electricity, such as voltage, current, frequency and phase, are converted to required specifications according to the intended application. The main function of power electronics is the conversion of such electrical features. Usually, this function is recognized as DC/DC, DC/AC, AC/DC, or AC/AC power conversion, and the electric power units for these purposes are called converters or inverters. The apparatus for which a converter/ inverter is used is typically divided into two types, motor and power supply. The former generates physical movement, and the latter provides electric energy with a given specification to another apparatus for its operation. For both types of apparatus, the utilization of an inverter makes their efficient and flexible operation possible through continuous output regulation without useless energy loss, which results in a great contribution to energy savings.

Compared with information processing and communication electronics, the fields where power electronics is applied through an inverter show quite a large variety (cf. Fig. 3). As a result, the required technical specification must cover a markedly wide range. For example, the voltage of power electronics apparatus ranges from several V to several tens of kV. Thus, in terms of the managed electric power capacity, the application field of power electronics is roughly classified into low-power, medium-power and high-power fields.

Electric power transmission/distribution, railway systems and industrial motor drive are categorized as the high-power field, where the managed power is greater than approximately 1 MW. This field has the significant aspect as

infrastructure, the required specifications for voltage and current capacity are extremely high, in addition to that for reliability. In the medium-power field of 1 MW–1 kW, there are many applications, such as distributed power supplies, local electric energy networks for buildings and homes, general-purpose motor drive, electric vehicles (EVs)/hybrid electric vehicles (HEVs), and household electric appliances. Because of the large total number of such apparatus in our society, the innovation of power electronics technology in this field remarkably contributes to solving the energy saving problem through the reduction of electric power loss and the miniaturization of power electronics apparatus. As the third category, the low-power field involving powers less than 1 kW includes switching power supplies for information technology (IT) or mobile apparatus, and inverters for lighting. On account of the recent trend to lower the operation voltage and increase the operation frequency of central processing units (CPUs), high current density and high current change ratio have become important factors in this field. Compared with the situation of other fields above, the cost as a total system is quite important for the spread of technological innovation.

2.2.2 Performance required for switching device for power electronics systems

The basic concept of electric power conversion in power electronics is digital switching. In Fig. 4, a comparison of DC/DC voltage regulations by a classical analog variable resistor and by a digital switching device is shown. In the former case, the output voltage is regulated by changing a variable resistor, and useless energy loss in the resistor cannot be ignored. The conversion efficiency often deteriorates, according to the output power. In contrast, the output is regulated on average by the ratio between the on- and off-times (t_{on} and t_{off}) of the electrical switch in digital switching. In this case, the energy loss in the circuit is quite small owing to a high-speed switching device and several passive elements that manage the energy flow averaging.

In digital switching, the low-energy loss feature of a switching device is an essential factor in energy conversion in the sense of minimizing energy loss, because the energy loss in the switching devices used is estimated to be 30–50% of the total energy loss of the conversion circuit. The

(a) Regulation by variable resistance (analog)   (b) Regulation by switching (digital)
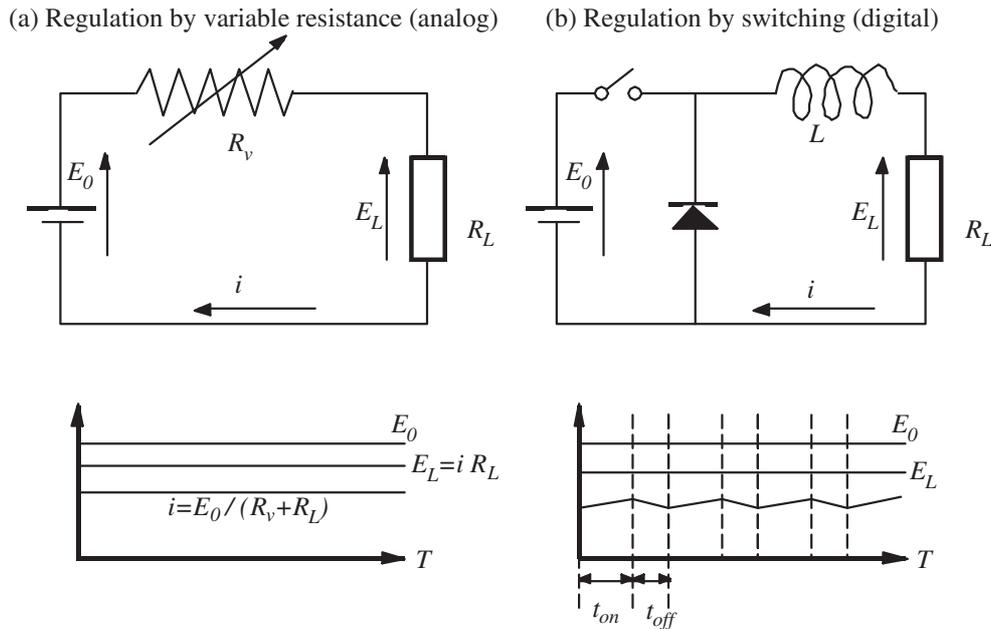
Fig. 4.   Two types of electric power conversion methods.

energy loss of a switching device is divided into conduction loss and switching loss. The former can be considered in terms of the resistance of a device itself. An ideal electrical switch is one that shows zero resistance at the on-state, and a resistance of infinity at the off-state. However, these two requests always have a trade-off relationship. In the electric power conversion, the handling of high voltage is often required, while the energy loss should be minimized as much as possible. From these requirements, switching devices are usually qualified by the indices of specific on-resistance and blocking voltage. On the other hand, the switching loss is determined to be proportional to the capacitance of a device and the operation frequency. Thus, the small capacitance of a device is also an important factor for a high-efficiency switching device.

From the viewpoint of a power conversion system, there is another requirement for the switching devices used. As mentioned above, a power conversion apparatus consists of switching devices and several passive elements, such as capacitances, inductances and filters. In most typical cases, the size of an apparatus is determined by these passive elements rather than the switching devices. By increasing the operation frequency, it is possible to reduce the size of the passive elements used, which results in the size reduction of the apparatus and the expansion of the utilization of power conversion apparatus. Therefore, the higher operation frequency is required as an important specification of a switching device in a power conversion apparatus. The operation frequency of the present main power switching devices, Si-GTO and Si-IGBT, is several hundred Hz– several kHz. There is a demand and an expectation for apparatus operating in the frequency range of several tens kHz to several MHz using majority-carrier devices made of novel widegap semiconductor materials.

Considering these low-loss and high-frequency features together, a new index of "power density W/cm^3" has been proposed to indicate the performance of a power conversion

unit. A clear increase in the power density is found in the trend of recent developments.[4)]

The requests for electric power switching devices used for power electronics are summarized as follows.

1. Higher blocking voltage, which enables the expansion of the utilization field and reliability.
2. Lower specific on-resistance, which enables the reduction in conduction loss in a device.
3. Higher operation frequency, which enables the reduction in apparatus size.
4. Lower capacitance, which enables the reduction in switching loss and the increase in operation frequency.

3.   Widegap Semiconductor Properties and High-Power Applications

Generally, covalent bond crystals composed of light elements on the second period of the periodic table are widegap semiconductors, which have characteristics of small bond length between constituent atoms and wide bandgap energy in comparison with Si and GaAs. In Fig. 5, the relationship between the bond length and bandgap energy of various kinds of semiconductor materials is shown. It is found that III–nitrides and SiC are located in a quite different domain from conventional elemental and compound semiconductors. Small bond length means that the bonding energy between constituent atoms is strong, and, as a result, the chemical stability of widegap semiconductor materials composed of light elements is extremely high. In addition, the large bonding energy and their small mass bring about large phonon energy, and it is difficult for lattice scattering to occur, which results in high thermal conductivity and high saturation drift velocity, macroscopically. On the other hand, it is also difficult for the avalanche effect to occur, owing to the large bandgap, and breakdown electric field becomes high. The large bandgap energy also contributes to the reduction in intrinsic carrier generation at high temperature and that in thermal current leakage at a junction,
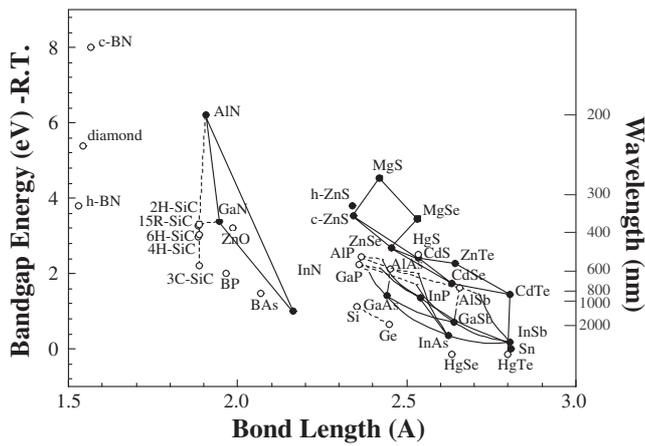
Fig. 5. Relationship between bond length and bandgap energy for various kinds of semiconductor materials.

which obstruct device operation. These characteristics are extremely attractive for high-frequency, high-power, high-voltage, high-temperature and low-loss operating specifications as semiconductor devices.

In Table I, the characteristic parameters of various semiconductor materials are shown. The parameter values of widegap semiconductor materials are very different from those of Si and GaAs. So-called figures of merit (cf. Table II[5]) composed of these parameter values have been so far proposed conventionally[6–10] as indices to express

whether individual materials are suitable or not for each application. For example, Keyes's index[7] is a suitable one for the high temperature operation of devices, while Baliga's index[8] expresses a low-loss feature. Baliga's high-frequency[9] index expressing a switching loss of a power FET, Johnson's index[6] expressing a frequency × power performance, and f_{max} as a HF operation limit are considered to be good indices for high-output power HF devices. Some of these values, such as breakdown electric field, have not been measured yet so accurately for widegap semiconductors, and the calculated value of an index somewhat changes depending on which parameter values are used for the estimation. At all events, widegap semiconductor materials exhibit large indices, and it is expected that an extremely superior performance is obtained when they are used for high-power device applications.

III–nitrides are III–V compound semiconductors as well as widegap semiconductors, and growth of mixed alloy and fabrication of heterostructure are possible. As a result, two-dimensional electron gas (2DEG) similar to that in AlGaAs/GaAs can be generated in terms of high carrier mobility, and a better performance is expected in actual HF device application. Furthermore, an extremely high sheet carrier density of $10^{13}/cm^2$ order can be easily generated in a AlGaN/GaN 2DEG system[11,12] by a spontaneous polarization along the {0001} direction and a piezoelectric polarization owing to the strain at the heterointerface as shown in Fig. 6, in comparison with a GaAs-related 2DEG

Table I. Important characteristic parameters of various kinds of widegap semiconductor materials for high-power device application.

Material	E_g (eV)	ε	μ_n (cm^2 V^{-1} s^{-1})	E_c (10^6 V/cm)	v_{sat} (10^7 cm/s)	κ (W cm^{-1} K^{-1})	Band type
Si	1.1	11.8	1350	0.3	1.0	1.5	I
GaAs	1.4	12.8	8500	0.4	2.0	0.5	D
c-GaN	3.27	9.9	1000	1	2.5	1.3*	D
h-GaN	3.39	9.0	900	3.3	2.5	1.3	D
3C–SiC	2.2	9.6	900	1.2	2.0	4.5	I
6H–SiC	3.0	9.7	370^a, 50^c	2.4	2.0	4.5	I
4H–SiC	3.26	10	720^a, 650^c	2.0	2.0	4.5	I
AlN	6.1	8.7	1100	11.7	1.8	2.5	D
Diamond	5.45	5.5	1900	5.6	2.7	20	I

a: along a-axis, c: along c-axis, *: estimate

E_g: bandgap energy, ε: relative dielectric constant, μ_n: electron mobility, E_c: breakdown electric field, v_{sat}: saturated drift velocity of electron, κ: thermal conductivity

Table II. Figures of merit of various kinds of widegap semiconductor materials for high-power device application.

Material	Johnson $(E_c v_{sat}/\pi)^2$	Keyes $\kappa(v_{sat}/\varepsilon)^{1/2}$	Shenai (Q_{F1}) $\kappa\sigma_A$	Shenai (Q_{F2}) $\kappa\sigma_A E_c$	Baliga $\varepsilon\mu E_c^3$	Baliga μE_c^2
Si	1	1	1	1	1	1
GaAs	7.1	0.45	5.2	6.9	15.6	10.8
c-GaN	685	1.5	20	67	23	8.2
h-GaN	760	1.6	560	6,220	650	77.8
3C–SiC	65	1.6	100	400	33.4	10.3
6H–SiC	260	4.68	330	2,670	110	16.9
4H–SiC	180	4.61	390	2,580	130	22.9
AlN	5,120	21	52,890	2,059,000	31,700	1,100
Diamond	2,540	32.1	54,860	1,024,000	4,110	470

σ_A = Shenai(Q_{F3}) = $\varepsilon\mu E_c^3$ (ref. 5).
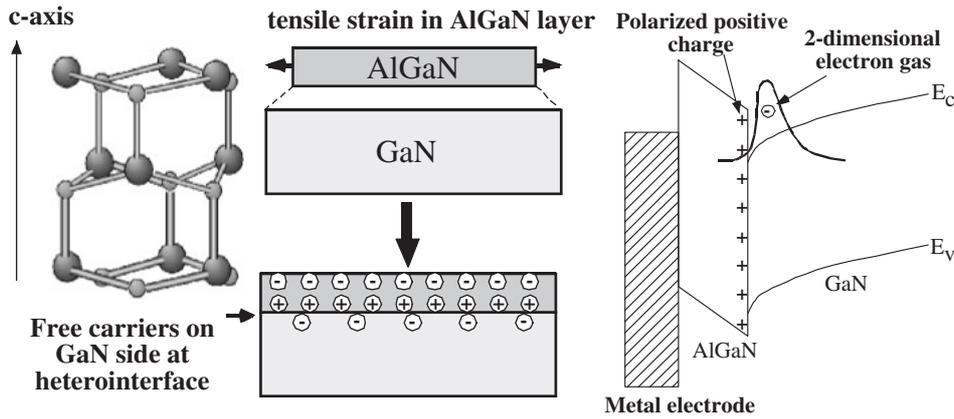
Fig. 6. AlGaN/GaN heterostructure and its band diagram. When the AlGaN layer is under tensile strain, free carriers are accumulated at the heterointerface owing to the piezoelectric effect caused by the strain, and a spontaneous polarization effect.

system. This high sheet carrier density is extremely profitable to high-current-capacity device operation. A GaN-related 2DEG system exhibits a sheet carrier density one order of magnitude higher than a GaAs-related system, although its mobility is inferior. Therefore, we can expect a comparable performance with a pseudomorphic high electron mobility transistor (p-HEMT) on InP in terms of sheet resistance.

4. High-Power Device Operation by Widegap Semiconductors

Even if we try to realize the high-performance system mentioned above, a limit is found in device performance owing to the material property limitations, and a practical system cannot be constructed as long as semiconductor devices made of conventional materials are used. Below, I discuss the strategy for overcoming the problems using widegap semiconductor devices.

4.1 Frequency and output power

Figure 7 schematically shows the output/frequency limit of HF device operation.[13] The obstruction of semiconductor device operation by heat generation limits the output power in region I, and a current amplification gain gives a limit to the performance in region III. On the other hand, the product

of output power and operation frequency is limited by that of the saturation drift velocity of carriers and breakdown electric field in region II. As for Si devices, high output power is rather possible in terms of a specific thermal conductivity compared with the case for GaAs; however, the electric current amplification gain suddenly falls in the region of frequencies greater than 1 GHz owing to lower mobility. For the expansion of region III, an improvement in mobility and finer device patterning are necessary, and it is known that HEMTs and heterojunction bipolar transistors (HBTs) based on GaAs have been developed. Furthermore, InGaAs and InP devices having higher mobility have been also developed. Above all, in region II, the characteristics of widegap semiconductors bring about an outstanding effect in order to exceed a device operation limit.[14] Thus, the approach of using novel materials exhibiting a large product value of carrier saturation drift velocity and breakdown electric field is believed to be quite important for the development of a new semiconductor device function in the future.

Meanwhile, we must consider several factors necessary to realize high output power under HF operation in FETs. Because high-speed operation is basically dominated by the velocity of carriers moving in a channel, a large drift velocity of carriers is the most important factor. On the other hand, a short gate length is required owing to the necessity to make gate capacity small, because parasitic capacitance greatly influences the response characteristics of a device in actual operation. However, as a result of shortened gate length, the electric field strength becomes large, assuming that the applied voltage between source and drain electrodes is constant. If the breakdown electric field of the semiconductor material used for a FET is small, the voltage available between source and drain inevitably shrinks for a shorter gate length. In other words, the smallest gate length is determined by the breakdown electric field of the material used for a given operation voltage, and higher-speed operation cannot be expected by the reduction of gate length. For example, a source–drain voltage of 20 V gives an electric field strength as high as 1×10^6 V/cm for a gate length of 0.2 μm, and brings about a breakdown for a GaAs device. Under low-electric-field operation, carrier mobility is a good material characteristic index for device operation.
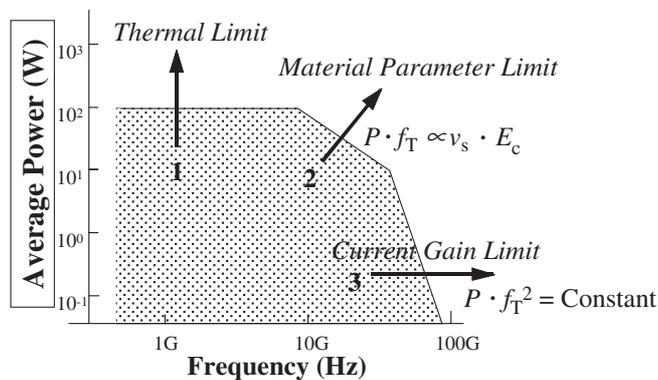
Fig. 7. Restrictions of HF devices in terms of output power and frequency. The limiting factors for HF device operation are thermal restriction, material property restriction and current gain restriction, for the respective regions shown in the figure.
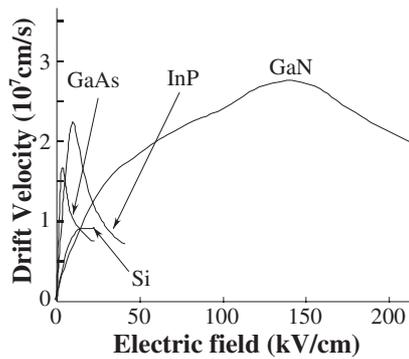
Fig. 8. Dependence of drift velocity of semiconductors on electric field. GaAs and InP have high mobilities (slope of drift velocity–electric field relation in the low-electric-field region); however, their drift velocities decrease in the high-electric-field region. On the other hand, GaN shows high drift velocity in the high-electric-field region.

However, drift velocity is more essential than mobility, that is a differential coefficient of a drift velocity–electric field strength relation under high electric field operation, and the saturation drift velocity becomes a more important index. The saturation drift velocity is quite large for GaN and SiC, and it is noted that the electric field strength needed to reach the saturation drift velocity is nearly one order of magnitude larger than that for GaAs, as shown in Fig. 8. Under this situation, we can make the best use of this high drift velocity value under a high electric field strength based on fine patterning structures. For GaAs and InP, the drift velocity rather decreases under an electric field strength of 10^5 V/cm. From these viewpoints, GaN and SiC, which exhibit high saturation drift velocities and large breakdown electric fields, are the most suitable materials that enable us to realize the ultimate short-channel device in which the operation with a high voltage between source and drain is possible for high-speed operation.

On the other hand, the output power of FET P_{out} is almost proportional to the product of drain current I_d and source–drain voltage V_{sd} (cf. Fig. 9). Therefore, to obtain the higher output power, we should consider the increases in I_d and V_{sd} primarily. Concerning V_{sd}, a breakdown voltage of several 10 V is easily obtained for a GaN device owing to its high

breakdown electric field, whereas the breakdown voltage of a GaAs metal–semiconductor field effect transistor (MESFET) is approximately 20 V at maximum. Here, the superiority of widegap semiconductor clearly appears. Furthermore, I_d is also proportional to the product of carrier density and drift velocity; a mobility of $1500–2000$ cm^2 V^{-1} s^{-1} and a sheet carrier density of 2×10^{13}/cm^2 are simultaneously obtained for the 2DEG system using hexagonal III–nitrides, owing to spontaneous polarization and piezoelectric polarization induced by strain as well as large band discontinuity. The latter high sheet carrier density is almost one order of magnitude higher than that obtained using GaAs-related materials. These phenomena indicate that the characteristics of widegap semiconductors, especially III–nitride heterostructures, are highly advantageous for both the factors that bring about high output power in FETs, and consequently enable the realization of high-power HF devices whose performance surpasses those of Si and GaAs HF devices.

4.2 Blocking voltage and specific on-resistance

In Fig. 10(a), the basic structures of power switching devices are shown. Each structure mainly consists of a channel that switches current flow and a drift layer that blocks applied voltage. The switching channel is usually controlled by the expansion of a depletion layer to the drift layer from several types of junctions. The electric field in the drift layer is illustrated in Fig. 10(b). An avalanche breakdown occurs when the electric field at the junction reaches the breakdown electric field E_c of the material used. Then, the blocking voltage of a device V_B is approximately determined as the area size below the curve indicating the electric field in Fig. 10(b), i.e., $(E_c \cdot W_D)/2$, where W_D is the necessary drift layer width. On the other hand, the specific on-resistance of the drift layer R_{DS} is expressed as $R_{DS} = W_D/(q\mu_n N_D) = 4V_B^2/(\varepsilon \mu_n E_c^3)$, where q is the electron charge, μ_n the electron mobility, N_D the donor density, ε the specific dielectric constant, and the denominator of the right side is Baliga's figure of merit. The donor density N_D is also expressed as $N_D = (\varepsilon/q) (E_c/W_D) = 2\varepsilon E_c^2/qV_B$. From these formulae, it is found that a material having high E_c and high μ_n is essential in order to obtain both low R_{DS} and high

Under Class A amplification,
$P_{out} = (1/8) \cdot (V_B - V_{knee}) \cdot I_{max}$

$I_{max} \sim n_s \cdot \mu$
$V_B \sim E_C$

Under I_{max}=1A/mm, V_B=80V (V_{sd}=40V), and W_g=20mm,
P_{out}=10W/mm and P_{total}=200W are obtained.
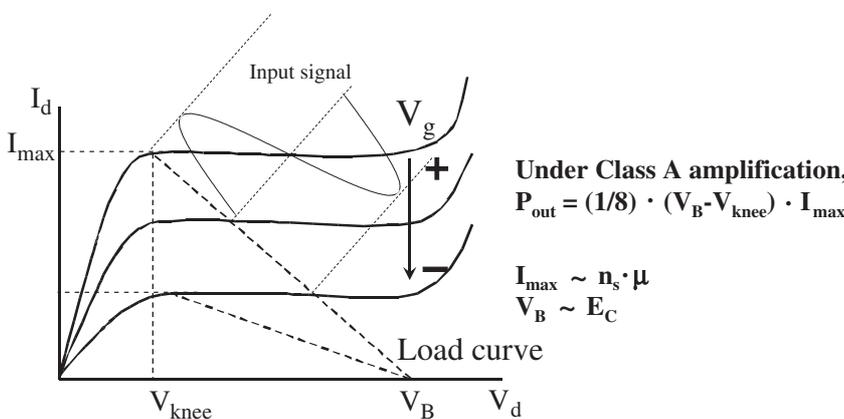
Fig. 9. Operation of high-power HF FET. I_d, V_d, and V_g are the drain current, drain voltage, gate voltage, respectively. V_{knee} is the knee voltage. The dashed line indicates a load curve. V_B and I_{max} are the drain voltage and maximum drain current under operation, respectively. V_B is determined by the breakdown electric field of the semiconductor material used, and I_{max} is proportional to the sheet carrier density and mobility at the channel.

Fig. 10.   (a) Basic structure of vertical power switching devices. (b) The electric field in the drift layer is shown. The difference between a Si device and a widegap semiconductor (WGS) device is illustrated. The slope is determined by each donor density N_D.

V_B. Comparing Si and SiC devices, an SiC drift layer can be doped more than approximately 100 times higher and its width can be 1/10 times thinner than those in the Si case, assuming the same blocking voltage. This higher doping indicates a marked reduction in R_{DS}. Finally, R_{DS} is inversely proportional to the third power of E_c, under the same blocking voltage. Therefore, the usage of widegap materials with large breakdown electric field is greatly profitable to the performance improvement of power switching devices.

For the specific on-resistance of an actual device R_{on}, channel resistance R_{ch} and contact resistance R_c, which are constant against the blocking voltage, are usually added. The relationship between V_B and R_{on} for various materials and R_{ch} is shown in Fig. 11. It is found that R_{DS} is dominant for the higher-voltage region, whereas R_{ch} determines R_{on} for the lower-voltage region. This situation would distinguish the advantageous regions of III–nitride and SiC devices, because the R_{ch} values of these two kinds of devices are quite different from each other. More precise evaluation of R_{on} was also carried out for a lateral-type switching device structure.[15]

On the other hand, the switching loss is proportional to the product of device capacitance, the square of applied voltage and switching frequency. It should be noted that the switching loss increases with increasing operation frequency and applied voltage. Finally, the total power loss density P_{total} is expressed as $P_{total} = (1-D)I_{on}^2 R_{on} + C_{iss}V_g^2 f + AC_{oss}V_{sd}^2 f$, where D is the duty ratio of switching, I_{on} the drain current at on-state, C_{iss} the input capacitance of a device, V_g the gate voltage, f the switching frequency, C_{oss} the output capacitance of the device, and A a constant specific to a given circuit. Because there are many factors
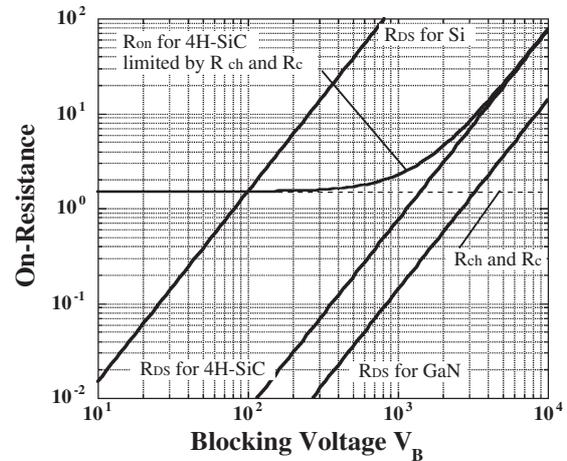
Fig. 11.   Basic relationship between V_B and R_{on} for switching device for various materials and R_{ch} values R_{on} is expressed as $R_{on} = (4\varepsilon\mu_n E_c^3)V_B^2 + R_{ch} + R_c$.

that determine the total power loss, it should be individually estimated appropriately for a given specification.

4.3   Heat dissipation

The heat generation problem always accompanies the high-output-power operation of a device. However, as characteristics of widegap semiconductors, large built-in potential or band discontinuity at a given junction enables high-temperature operation. Such a device exhibits not bad performance even if there is an internal temperature increase induced by heat generation. In addition, SiC has quite a high thermal conductivity, and it is extremely profitable to heat dissipation when it is used as a substrate. Concerning GaN,

its specific thermal conductivity has been so far considered to be lower than that of Si, and is a weak point for heat dissipation. Recently, it has been reported that the specific thermal conductivity of high-quality GaN crystals shows a larger value of greater than $2\,\mathrm{W\,cm^{-1}\,K^{-1}}$,[16,17] as a result of recent advances in bulk crystal growth.

Thus, the characteristics of widegap semiconductor materials, such as high saturation drift velocity, high breakdown electric field, high specific thermal conductivity, and high temperature stability, are believed to be great advantages for the fabrication of high-power devices.

5. Present Status of Widegap Semiconductor Power Devices

Widegap semiconductors have several superior material properties suitable for the high-power performance of HF or low-loss switching devices as mentioned above. On the other hand, their strong chemical bond has an adverse effect, and their crystal growth and device fabrication were extremely difficult. However, according to recent developments in material processing technology, various kinds of device structures have been fabricated since the 1990s. In the case of GaAs MESFET, which is a representative HF device at present, the upper limit of operation voltage is less than 20 V, and the maxima of output power and power density for a single-device chip are estimated to be approximately 20–40 W and 1 W/mm, respectively. Recently, superior device performance surpassing these values has been reported successively. The present development status of these high-power devices based on SiC and III–nitrides is presented below.

5.1 High power HF devices
5.1.1 Silicon carbide

Using SiC, the realization of HF devices with output powers of several 10 W–several kW (output power density of several W/mm) is expected for the frequency range from 10 MHz to several GHz, and devices such as MESFETs, static Induction transistors (SITs), junction FETs (JFETs) have been fabricated. In the case of MESFETs, the microfabrication process is easy, which is the most attractive advantage for HF applications. JFET is considered suitable for high-temperature operation owing to its p–n junction structure; SIT, which has a vertical-type structure, is more suitable for large current applications. Recently, 4H polytype has been mainly used for MESFET because of its lower anisotropy and higher mobility than 6H–SiC, and output power densities higher than 3 W/mm as well as current gain cut-off frequencies f_T higher than 20 GHz have been achieved with a submicron gate length. An HF performance of $f_T = 22\,\mathrm{GHz}$, a maximum oscillation frequency of $f_{max} = 50\,\mathrm{GHz}$[18] with a gate length of $L_g = 0.45\,\mathrm{\mu m}$ and a gate width of $W_g = 250\,\mathrm{\mu m}$, $f_{max} = 42\,\mathrm{GHz}$[19] with $L_g = 0.7\,\mathrm{\mu m}$, and $W_g = 32\,\mathrm{\mu m}$, an output power density of $3.3\,\mathrm{W/mm}$ (850 MHz), a power added efficiency of 66.7%[20] have been reported. An output power density of 7.2 W/mm (3 GHz)[21] was also reported using semi-insulated substrates. As for the total output power, a 120 W pulsed output and an 80 W CW output were achieved by 3.1 GHz operation.[22,23] In addition, $f_T = 7.3\,\mathrm{GHz}$, $f_{max} = 9.2\,\mathrm{GHz}$, a power density of $1.3\,\mathrm{W/mm}$ (850 MHz), operation up to a temperature of 873 K were

confirmed for 6H–SiC devices.[24] In the case of JFET/SIT structures, a device with a high output power of 450 W (1.3 W/mm, 90 V operation) was also realized at 600 MHz,[25] which reaches the level of practical use. A transmitter module for the UHF band has been already fabricated, and a peak output of 1 kW was demonstrated.[26] In addition, Sriram *et al.* performed a lifetime test at a junction temperature of 240 °C using an SiC MESFET, and they reported a linear gain degradation of 0.3 dB and a saturation power degradation of 0.4 dB even after 700 h operation, which means that the device reliability does not have any problem.[27] Besides these types of devices, the fabrication of an impact ionization avalanche transit-time (IMPATT) diode was also reported with a peak output power of 1.8 W (11.8 GHz), aiming at applications in the millimeterwave region.[28]

5.1.2 III–nitride semiconductors

As for electron devices using III–nitrides, an HFET structure that utilizes a 2DEG system, as well as a MESFET, has been mainly fabricated. Nowadays, not only performances such as an f_T of 60–120 GHz, an f_{max} of 100–150 GHz, a transconductance g_m of 300–400 mS/m, and a maximum drain current I_{dmax} of 1–1.5 A/mm have been obtained without considerable difficulty, but also high output powers of several W in the millimeterwave region, and several hundreds of W (up to several tens of W/mm as output power density) in the microwave region have been demonstrated.[29–31] It can be said that a superior HF performance level that has never been provided with GaAs devices has been realized.

A MESFET using an undoped n-type GaN layer grown by metal organic vapor phase epitaxy (MOVPE) method was first fabricated experimentally in the first half of the 1990s,[32,33] demonstrating a g_m of 20 mS/mm with a gate length of several μm, and $f_{max} = 17\,\mathrm{GHz}$ as its HF characteristic. However, a major trend of device development has afterwards shifted to the utilization of 2DEG, taking advantage of the characteristics of III–V group compound semiconductors. The existence of 2DEG in the AlGaN/GaN system was found for the first time in 1991 by Khan *et al.*,[34] as an outstanding increase in mobility. Afterwards, the Shbnikov de Haas oscillation and the quantum Hall effect were confirmed,[35] and mobility as high as several thousand $\mathrm{cm^2\,V^{-1}\,s^{-1}}$ and sheet carrier density on the order of 10^{12}–$10^{13}/\mathrm{cm^2}$ were realized at low temperature.[11,36–38] So far, mobilities higher than 50,000 $\mathrm{cm^2\,V^{-1}\,s^{-1}}$ have been reported at cryogenic temperature.[39,40]

An HFET device that uses these 2DEG systems was realized for the first time in 1993.[41] In this report, the obtained performance was $g_m = 27\,\mathrm{mS/mm}$ (RT), 46 mS/mm (77 K) with a 4 μm gate length; however, quite a number of HFET fabrication attempts have successively followed it afterwards, and the DC and HF performances have been markedly improved, using various device fabrication techniques. In addition to these studies, investigations concerning high-power performance under HF operation have also started. Reports demonstrating CW output power densities higher than 1 W/mm appeared successively after the first report of 0.3 W/mm at 10 GHz,[42] which exceed the high-

(a)

(b)
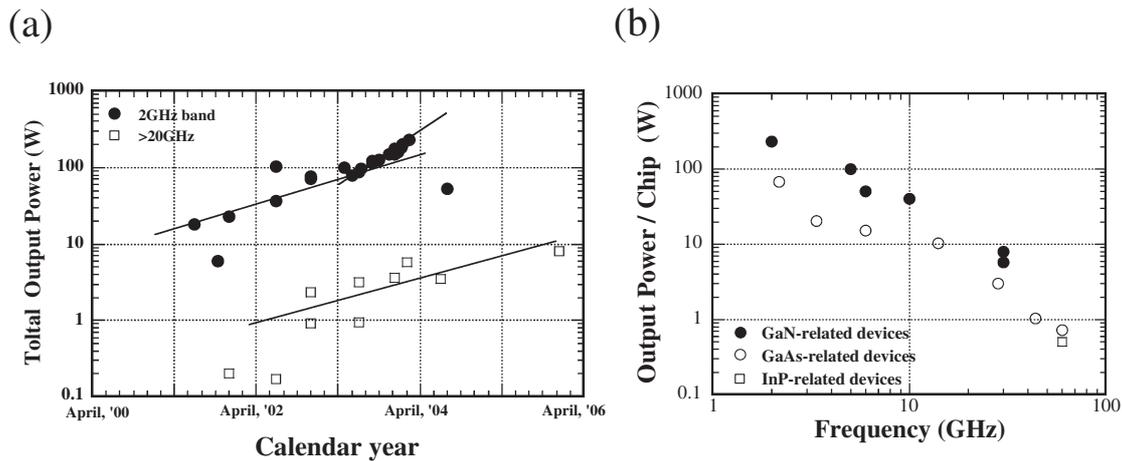
Fig. 12.   (a) Recent progress in output performance of AlGaN/GaN HF HFET in 2 GHz band and millimeterwave band beyond 20 GHz.
(b) Relationship between reported maximum output power and frequency.

power performance of GaAs devices. In particular, the output power of 1 W was realized by adopting SiC substrates instead of sapphire, to solve the heat dissipation problem.[43–45] The present highest performance is described below.

Concerning DC characteristics, a g_m higher than 500 mS/mm obtained using a recess structure was reported.[46] As for HF performance, $f_T = 110$ GHz, $f_{max} = 140$ GHz with $L_g = 50$ nm,[47] $f_T = 121$ GHz, $f_{max} = 162$ GHz with $L_g = 0.12$ μm,[48] $f_T = 152$ GHz, $f_{max} = 173$ GHz with $L_g = 60$ nm,[49] and $f_T = 81$ GHz, $f_{max} = 187$ GHz with $L_g = 90$ nm[50] are the best ones. A drift velocity of approximately 1.8×10^7 cm/s was estimated from the f_T value. Considering these recent development, further improvement beyond $f_{max} = 200$ GHz can be well expected.

Concerning output power density, values of 2.8 W/mm (8 GHz), 2.6 W/mm (10 GHz) with $L_g = 0.7$ μm,[51] and 6.6 W/mm (6 GHz) with $L_g = 0.4$ μm, $W_g = 100$ μm[52] were reported for devices on sapphire substrates. In terms of the power density, the larger thermal conductivity of substrates is so critical; power densities of 11.2 W/mm (10 GHz, 45 V operation) with $L_g = 0.3$ μm, $W_g = 100$ μm,[53] and as high as 32.2 W/mm (4 GHz, 120 V operation) were achieved using SiC substrates.[54] In the Ka band (20–40 GHz band), values of 5 W/mm (26 GHz) with $L_g = 0.25$ μm, $W_g = 200$ μm,[55] 7.9 W/mm (30 GHz) with $L_g = 0.25$ μm, $W_g = 360$ μm,[56] and 2.32 W/mm (35 GHz)[57] were also reported. These output density values are more than 10 times higher than those of AlGaAs/GaAs HEMTs.

The recent progress of output power itself is also remarkable. Even on sapphire substrates, 7.6 W ($W_g = 6$ mm) using the flip-chip technique[58] and 22.6 W ($W_g = 16$ mm) using the substrate thinning technique[59] were realized. On SiC substrates, 9.8 W (8.2 GHz)[60] with $L_g = 0.6$ μm, $W_g = 2$ mm, and 38 W (10 GHz)[61] with $L_g = 0.4$ μm, $W_g = 12$ mm were demonstrated in the 1990s. Since 2001, reports demonstrating output powers greater than 100 W have appeared, i.e., a 113 W pulsed output on a thinned sapphire substrate,[59] and a 103 W (2 GHz, 50 V operation) CW output.[62] Most recently, a single-chip output of 230 W (2 GHz, $W_g = 48$ mm),[63] and 2-chip output of 250 W[64] have been achieved. These high output powers are much

attributed to the improvement of device structures, such as the recess gate, field plate, and n-type GaN cap layer and so on. In addition, it is also notable that a pulsed output power of as high as 368 W in the L band on Si substrates was announced.[65] Even in the 30 GHz band, 5.8 W[50] and 8 W[66] HF output powers have been reported successively. The recent progress of the output performance of AlGaN/GaN HF HFETs and the reported maximum output power in terms of frequency are shown in Fig. 12.

In addition to the normal AlGaN/GaN HFET structure, there have been also several attempts of insulated-gate HFETs (MISHFETs). Not only $g_m = 235$ mS/mm with an AlN layer,[67] but also an excellent HF performance of $f_T = 70$ GHz and $f_{max} = 90$ GHz ($g_m = 193$ mS/mm, $I_d = 1.3$ A/mm at $L_g = 0.1$ μm) with an Al_2O_3/Si_3N_4 doublelayer[68] was reported. A high-power MISHFET performance of 141 W at 2 GHz was also demonstrated.[69] Furthermore, there have been several reports on HBT structures. A GaN/SiC structure was attempted by Pankove and coworkers,[70,71] aiming at improving the emitter efficiency using widegap materials as an emitter. A current gain of 10,000,000, and an extremely large current density of 1,000 A/cm² were shown. In addition, npn HBTs having an AlGaN/GaN[72–74] or GaN/InGaN[75,76] structure have been recently fabricated. A breakdown voltage of 450 V, a current gain of 3,000, an offset voltage of 1 V, a current density of 6.7 kA/cm² and an output density of 270 kW/cm² were reported owing to the reduction of p-type base layer resistance and the regrowth of an outer base layer; however, several points still remain to be improved, such as the device structure and fabrication process. A trial using InGaN as a channel layer was also made to realize markedly higher mobility, and a performance of $f_T = 153$ GHz and $f_{max} = 230$ GHz with $L_g = 0.16$ μm was reported.[77]

5.2 High-power switching devices
5.2.1 Silicon carbide

Aiming at applications in power electronics, several types of SiC electron devices have been fabricated so far, including PiN diodes, Schottky barrier diodes (SBDs), MOSFETs and JFETs. Compared with that of the transistors, the development of these 2 types of diodes has made an

earlier lead. From the difference in on-voltage V_{on} caused by the intrinsic built-in potential at the junction, SiC SBD can be used for the voltage region below approximately 4 kV exhibiting small on-resistance, whereas the SiC PiN diode shows its advantage for the higher-voltage region where its high V_{on} can be ignored. The excellent performance of SiC SBD has been already proved by several reports, such as $V_B = 2.22$ kV with $R_{on} = 2.5$ V,[78] $V_B = 4.15$ kV with $R_{on} = 9.07$ V,[79] and $V_B = 10$ kV with $R_{on} = 6$ V,[80] and so on. Also, a current capacity of 100 A was achieved with a yield of 79%.[81] Thus, SBDs with a blocking voltage of 300–1200 V and a current capacity of several A have been already commercialized, and they show extremely small recovery switching loss. Concerning the SiC PiN diode, the degradation of V_{on} under large-forward-current operation was once reported.[82] This phenomenon turned out to be associated with the expansion of stacking faults triggered by a basal plane dislocation, and can be suppressed using high-quality epitaxial wafers.[83,84] Thus, an excellent high-voltage performance of $V_B = 19.5$ kV with $R_{on} = 6.5$ V has been reported.[85] Also, a large current capacity of 100 A with $V_B = 5.2$ kV, $V_{on} = 4.2$ V,[85] or 50 A with $V_B = 10$ kV, $V_{on} = 4.2$ V[86] was demonstrated using a large chip size of 6 or 8.5 mm□, respectively. Because the PiN diode does not show any increase in on-resistance or leak current at high temperature as observed for SBD, there is an expectation for high-temperature use.

As a power switching device, the mainstream of the development is vertical-type normally-off MOSFET, on account of its ease of use and its wide application area. Among the polytypes of SiC, 4H–SiC has been mainly used, and its higher mobility and breakdown field along the {0001} crystal axis is preferable for a vertical device structure. At the early stage, the specific on-resistance of SiC MOSFET was not so reduced as expected from material properties, mainly due to its poor channel mobility. This situation would make the competition against Si super-junction devices[87] extremely severe. However, recent developments in device processing technology have enabled the realization of specific on-resistance values less than 10 mΩ cm² for a 600–1200 V blocking voltage design,[88–90] which are comparable to that of Si superjunction devices. Besides conventional double diffused MOSFET (DMOS-FET) and U-shaped trench MOSFET (UMOSFET), various modifications have been tried, such as accumulation FET (ACCUFET), epi-channel FET (ECFET), static induction injected accumulated FET (SIAFET), static channel expansion MOSFET (SEMOSFET), delta-doped accumulation channel FET (DACFET), double Epitaxial MOSFET (DE-MOSFET), implantation and epitaxial MOSFET (IEMOS-FET) varying in terms of MOSFET structure and fabrication process. Most recently, our group has achieved a specific on-resistance value as small as 2.7 mΩ cm² with a blocking voltage of 700 V by using the original structure of IEMOSFET.[91] For the higher-blocking-voltage region where SiC device can exhibit a distinct advantage, there have been also markedly low specific on-resistance values, such as 15.7 mΩ cm² with 1400 V,[92] 13.5 mΩ cm² with 2,300 V,[93] 45 mΩ cm² with 3,000 V,[94] and 88 mΩ cm² with 5,020 V.[95]

Concerning JFET, intensive effort has been also made.

The JFET structure is another type of switching device structure and is free from the oxide interface problem to be mentioned later. Several excellent performances have been reported in the past few years, such as 1.01 mΩ cm² with 700 V,[96] 10 mΩ cm² with 1,200 V, 25 mΩ cm² with 3,300 V[97] using a buried-gate structure, 218 mΩ cm² with 5,500 V[98] with an static expansion channel JFET (SEJFET) structure, 106 mΩ cm² with 10 kV,[99] and 3.6 mΩ cm² with 1,726 V[100] with a trench-type structure showing normally-off characteristics. These on-resistance performances of JFET generally surpass those of MOSFET. However, JFET usually shows only normally-on characteristics, and attempts to make it normally-off have been carried out by precise fine-patterning of the channel.

Besides the unipolar switching devices mentioned above, there have been also several reports using a bipolar structure, aiming at lower on-resistance or higher blocking voltage. In these cases, current gain β and current capacity are other important factors. On-resistance values of 6.0 mΩ cm² with 1,000 V (30 A capacity, $\beta = 40$),[101] 5.3 mΩ cm² with 1,400 V (17 A capacity, $\beta = 14$)[102] and 12 mΩ cm² with 1,750 V (4.9 A capacity, $\beta = 25$)[103] have been reported. For the higher-voltage region, a blocking voltage of 12.7 kV with $V_{on} = 6.6$ V was reported using an SiC commutated gate turn-off Thyristor (SICGT) structure.[104]

In Fig. 13, the specific on-resistances of unipolar and bipolar switching devices reported so far are plotted against their blocking voltage, including those of GaN HFET devices, which will be described later. In addition to the efforts to reduce on-resistance and enhance blocking voltage, the development of devices that can handle a current capacity as high as several tens of A will increase in necessity in the future, under the situation that the current capacity of SiC switching devices still remains so small compared with those of SiC diodes. Moreover, trials to install these devices in actual inverter modules and their evaluation have already begun.

5.2.2 III–nitride semiconductors

Because III–nitride wafers are heteroepitaxial ones, they
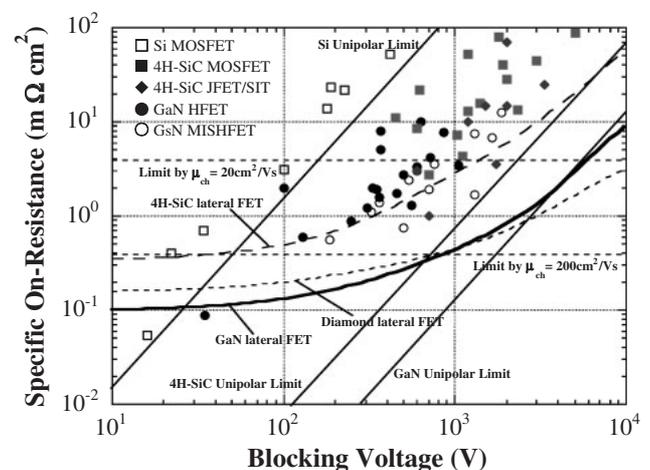
Fig. 13. Performance of power switching devices reported so far in terms of specific on-resistance R_{on} and blocking voltage V_B. The three curves denoted as lateral FET indicate the simulation results for the lateral structures obtained by Saito et al. (ref. 15).

were previously believed to be inappropriate for high-voltage switching applications due to their large number of crystal defects contained, especially threading dislocations. However, their 2DEG characteristics are quite preferable for obtaining low channel resistance and high switching speed. The GaN bulk feature exhibits a large breakdown electric field comparable to that of SiC. If the crystal defects do not considerably affect the breakdown tolerance, even higher blocking voltages can be expected for the AlGaN/GaN HFET structure. In addition, the most significant difference between a typical SiC switching device and an AlGaN/GaN HFET is in the structure, i.e., the former has a vertical-type structure, whereas the latter has a lateral-type structure. The relationship between specific on-resistance and blocking voltage was precisely simulated for the lateral device structure by Saito *et al.*, and sufficiently low specific on-resistance was found to be achievable, especially in the low-blocking-voltage region lower than several 100 V.[15] This lateral structure of AlGaN/GaN HFET would be also advantageous in terms of low switching loss owing to small device capacitance as well as the possibility of planar integration. Thus, since the first demonstration of the performance as a switching device using an AlGaN/GaN HFET structure in 2001,[105] several attempts have been made to realize high-blocking-voltage, large-current or low-on-resistance characteristics based on AlGaN/GaN HFET structures. The above report demonstrated a performance of $V_B = 1,050$ V with $R_{on} = 3.4$ mΩ cm^2, and several reports in the blocking voltage range of 600–1000 V followed the first one.[106,107] To date, better performances of $V_B = 1.3$ kV with $R_{on} = 1.7$ mΩ cm^2 using an SiN/SiO$_2$ gate insulator,[108] and $V_B = 1.7$ kV with $R_{on} = 6.9$ mΩ cm^2 using an SiN gate insulator[109] have been reported, by adopting sufficient source–drain distance. An example of their high voltage DC characteristics is shown in Fig. 14. Our group also demonstrated a high blocking voltage performance of 1.9 kV,[109] and a low on-resistance of 0.089 mΩ cm^2.[110] These performances are far superior to those of SiC switching devices, although all these characterized AlGaN/GaN HFETs show only normally-on characteristics. As in the case of SiC devices, electric power conversion systems request further improvements in current capacity; large current demonstration as high as 20 A[111] and 150 A[112] have been already reported.
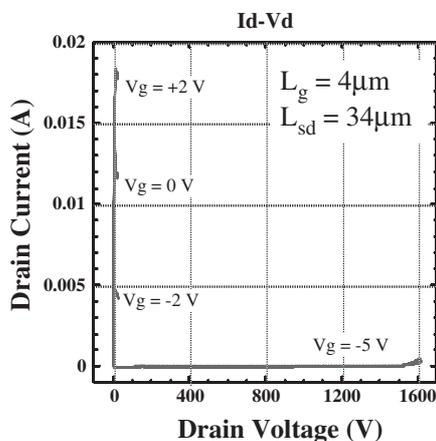
Besides the HFET structure using 2DEG, there have been several attempts by other types of device structures. The first one is a MOSFET using an undoped GaN layer with an oxide layer instead of a 2DEG system.[113] Although its channel mobility was as low as 45 cm^2 V^{-1} s^{-1}, the normally-off operation with $V_{th} = 2.7$ V was observed. The other is a vertical-type structure using a 2DEG channel and a conductive GaN substrate.[114]

6. Technological Problems for Future Research and Development

Because widegap semiconductor materials show quite large values of breakdown electric field, saturation drift velocity, and specific thermal conductivity as well as high-temperature stability as described above, they are expected to enable device operation at a higher output power than Si and GaAs. The basic structures of SiC MOSFET and AlGaN/GaN HFET are shown in Fig. 10(a). Concerning the component processing technology for their fabrication and the overall performance, the recent progress in the past several years is outstanding; however, peculiar problems as an electron device have been identified, without arriving at the stage where we can make best use of these superior material properties. These problems are in most cases common to HF and switching devices, and it is thought that further technology development is necessary. Below, the technological issues that need to be solved in the future, which have become clear in the past research and development, are described, considering the requirements imposed by application fields.

6.1 Self-heating

To achieve the high output power of a HF device or to realize the high current capacity of a switching device, it is inevitable that the I_d and V_{sd} of a device become large at the time of device operation. However, as a result of drift velocity decrease and impact ionization coefficient increase under the temperature increase caused by carrier drifts along the channel, not only I_d and g_m decrease, but also V_B decreases, and high-output-power operation virtually becomes impossible. On this account, the efficiency of heat dissipation considerably affects the performance of a device at the time of high-power operation even for widegap semiconductor devices. In fact, many results have been reported that I_d decreases because of the temperature increase when a device works under high-power operation by increasing V_{sd} or I_d. On the contrary, further improvement in output power is thought to be still possible considering the performance expected from the material properties. Figure 15 shows simulated values[115] and experimentally measured data of output power density against V_{sd} for various types of HF devices. Output power densities of several W/mm, and 15 W/mm are expected for AlGaN/GaN HFET on sapphire and on SiC substrates, respectively, at operation voltages greater than 10 V. Although output power densities surpassing this simulation have been already achieved at an operation voltage greater than 100 V, the estimation from the viewpoint of this heat dissipation may

Fig. 14. Example of DC characteristic of AlGaN/GaN MISHFETs showing high blocking voltage greater than 1 kV with specific on-resistance of several mΩ cm^2. For this device, $V_B = 1.7$ kV and $R_{on} = 6.9$ mΩ cm^2.
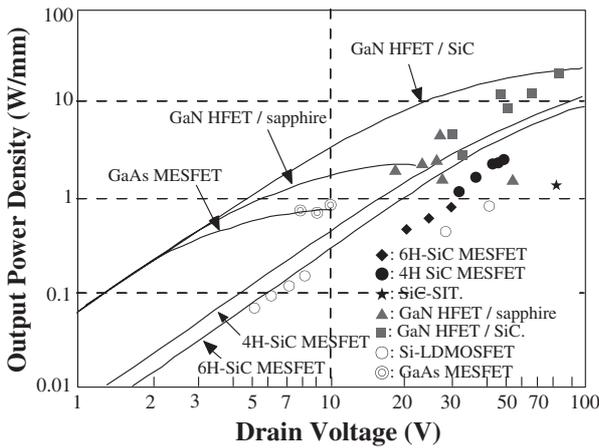
Fig. 15. Simulated values and actually measured data in terms of relationship between output power density and drain voltage for Si, GaAs, SiC, and GaN HF FETs.
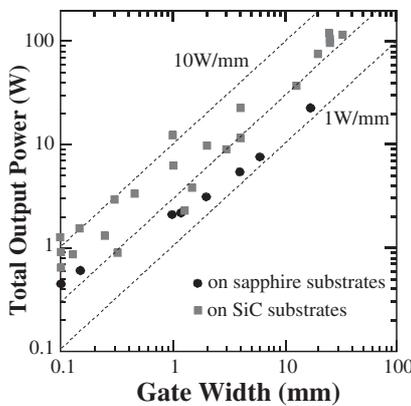
Fig. 16. Relationship between gate width and output power of AlGaN/GaN HFETs reported so far.

be one excellent index, for anticipating the future development. The use of SiC substrates, which is superior in terms of thermal conductivity, is essential for solving this heat dissipation problem. Moreover, technological developments such as thinning of substrates, flip-chip technology, via hole processing, and heat dissipation packaging for cooling are expected.

In addition, the relationship between gate width W_g and output power P_{out} for AlGaN/GaN HFET HF devices reported so far is shown in Fig. 16. For large peripheral devices, prospective output power density expected from the performance of small devices is not usually obtained. As a result, it is difficult to fabricate sufficiently high output power devices for practical applications. It seems that the weakest local region in the entire device structure determines the overall performance as a result of the poor uniformity of heat distribution, the inhomogeneity of chip characteristics in multicell structures or the inequality of HF input in large peripheral devices. For this improvement, it will be necessary to optimize device patterns in a way that considers the heat distribution as well as to realize homogeneous device processing and wafer characteristics. The development of characterization techniques such as

temperature measurements of a microdomain in an actual device structure is also important, for this purpose.

6.2 High-voltage operation and current leakage

For high-output-power and high-efficiency operation of HF FET, it is important to operate a device with a high V_{sd} value. As estimated from the material properties, operation with a V_{sd} as high as 100 V is possible; however, most reports have actually demonstrated operation at approximately 30–60 V, and 100 V for III–nitrides and SiC, respectively. In particular, the gate leakage current reaches as high as 10^{-3} to 10^{-2} A/mm^2 and the current leakage through the buffer layer immediately above the substrate sometimes deteriorates the pinch-off characteristic, for lateral III–nitrides devices. For the high leakage current of the AlGaN Schottky junction, the influences of factors such as Al content[116–118] have been reported, and several hypotheses have been proposed as the origin, such as the thin-surface-barrier model[119–121] and screw dislocation model,[122–124] however, the origin of the leakage has not been fully clarified yet.[125] These undesirable characteristics bring about the deterioration of the efficiency as well as the blocking voltage of a device. As a solution for the gate leakage, the MISHFET structure with an insulated gate is promising. As an insulating layer, high-dielectric-constant materials showing a low interface state density and a sufficiently high barrier effect are desirable; AlN,[126] Al_2O_3,[127,128] SiN,[129] and NiO[130] have been investigated besides conventional SiO_2. Figure 17 shows the difference in gate leakage characteristic between an AlN-MISHFET and a conventional HFET obtained by our group.[126] It is indicated that an insulated-gate structure is extremely effective for leakage current reduction, and it also works well for improving the blocking voltage[131] of high-power switching devices. Thus, a high blocking voltage greater than 1 kV for an AlGaN/GaN switching device was first realized only by the introduction of such a MISHFET structure. On the contrary, the introduction of an insulating layer sometimes results in an increase in interface trap density, which may be associated with the current collapse to be mentioned later. Thus, further examination is necessary for this and other issues, including the fabrication process and HF characteristics.

Furthermore, it is necessary to develop a process technology that enables the design and fabrication of device structures appropriate for high-voltage operation, in order to
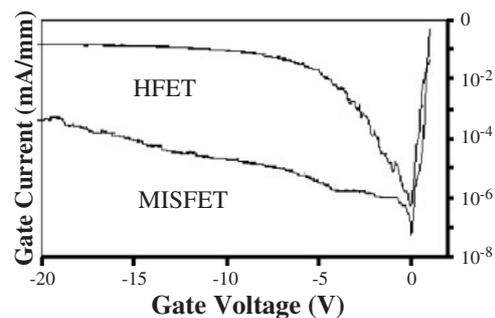
Fig. 17. Difference in the gate leakage characteristic between AlGaN/GaN–MISHFET with AlN layer and conventional AlGaN/GaN HFET (ref. 126).
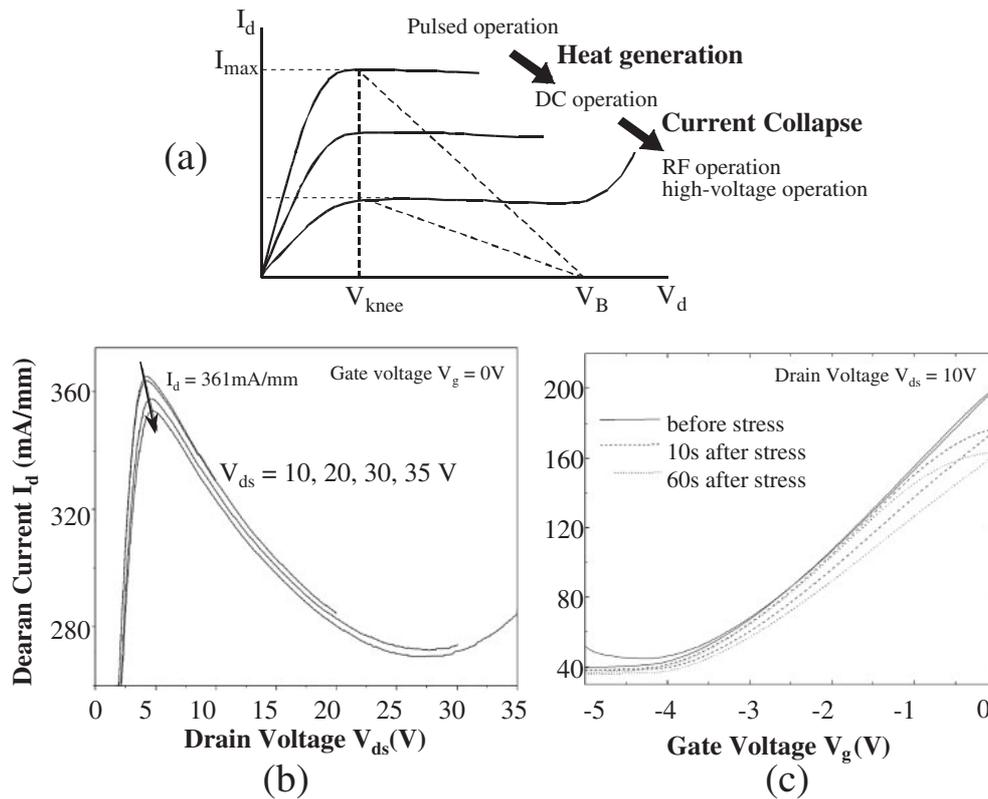
Fig. 18.   The deterioration of a HF device in different operation modes is schematically drawn, and actual examples of deterioration are also shown. Due to the stress of high-frequency, high-voltage or high-current operation, the drain current I_d decreases.

relax the electric field overconcentration in the vicinity of electrodes. In particular, this requirement is for operating small-size devices under a high electric field. The introduction of various field plate structures, which has been demonstrated to be effective for GaAs HF devices, has been attempted for AlGaN/GaN HFET,[132–134] and has contributed markedly to the improvement in HF output power. Also, the insertion of an n-doped GaN cap layer in an AlGaN/GaN HFET structure was found to be effective for a similar purpose.[64]

6.3   Current collapse

As shown in Fig. 18, the phenomenon in which the prospective I_d from the DC characteristic is not obtained at the time of high-voltage or HF operation is known for AlGaN/GaN HFET.[135,136] This phenomenon is called current slump or current collapse, and the participation of deep levels in the crystal or surface levels is implied.[137] There is also a report which attributes the origin to nitrogen vacancies;[138] however, no final conclusion has been found yet. It is supposed that the current reduction can be suppressed by surface passivation using SiN; however, the blocking voltage of a device seems to deteriorate in such a case. The simultaneous achievement of both the characteristics is important. In addition, there is an indication that the trap states existing in the substrate or at the interface between the substrate and the cannel bring about a variation in I_d for SiC HF devices.[139,140] It is needless to say that fundamental research regarding the elucidation of deep levels and surface traps, as well as the development of process technology for the passivation or treatment of the surface, is necessary. The problem of deep levels will be in particular an issue that we must clarify, in conjunction with crystal growth technology.

6.4   Channel mobility and reliability

For the performance improvement of SiC MOSFET, the most critical problem is the inferiority of the channel mobility at the SiO_2/SiC interface, especially for applications below 1,000 V. In contrast to the 4H–SiC bulk mobility of approximately $1,000\ cm^2\ V^{-1}\ s^{-1}$, the channel mobility of the SiC MOS structure remained at typically less than 10 $cm^2\ V^{-1}\ s^{-1}$ in the 1990s.[141] This low mobility is attributed to a significant number of trap levels at the interface. The existence of C clusters at the interface, or the association of O vacancies in the SiO_2 layer is implied for the origin of the trap level;[142] however, any conclusive evidence has not been shown. To improve the channel mobility, a great deal of effort has been made continuously throughout the world by various types of method, such as a modified oxidation process,[143] thermal annealing in H_2,[144] NO,[145,146] or N_2O[147] atmosphere, utilization of a crystal face other than (0001),[148] and adoption of a buried-channel structure.[149] As a result, a channel mobility higher than $200\ cm^2\ V^{-1}\ s^{-1}$ has been obtained nowadays;[150] however, this value is still low compared with the bulk value. Furthermore, after passing through various fabrication processes, the channel mobility is likely to decrease further. Considering these situations, further effort for channel mobility improvement is necessary.

Concerning device reliability, the gate oxide layer of the MOS structure is the primary objective. Compared with the

Si MOS structure, the SiO$_2$/SiC interface is imperfect and its band offset is smaller. In addition, higher-electric-field and higher-temperature operation are requested for SiC devices, and the influence of substrates cannot be ignored as will be mentioned later. These situations require higher reliability for SiC MOS devices. At the present stage, the reliability of the SiC MOS structure determined by time dependent dielectric breakdown (TDDB) evaluation remains at least one order of magnitude inferior to the equivalent Si MOS structure, and our group has studied the anticipated influence of dislocations on the reliability in detail.[151] The establishment of high reliability ensuring actual use is desired. For high-power high-frequency AlGaN/GaN HFET, similar high reliability is to be required, in the context of the installation to base stations of mobile telephone systems.

6.5 Normally-off characteristic

Different from the application to HF amplifiers, a switching application usually requires normally-off characteristics for a component switching device. In the case of SiC MOSFET, it is not so difficult to obtain normally-off characteristics by the adjustment of the device structure, although the device performance is slightly deteriorated compared with that of normally-on structures. However, precise control of the channel fabrication process is necessary for SiC JFET and AlGaN/GaN HFET. In particular, the piezoelectric field contributing to the high sheet carrier concentration in the channel works negatively for the realization of normally-off characteristics in the case of AlGaN/GaN HFET. Even if obtained, the threshold V_{th} is quite small on the positive side. It is thought that some breakthrough is necessary to realize reliable normally-off characteristics for these two types of devices. Actually, there exist several unique attempts for realizing normally-off characteristics; for example, by the introduction of fixed charges to the AlGaN barrier layer,[152] by utilizing a non-polar crystalline face that avoids the piezoelectric field, by utilizing an AlInN barrier for strain control,[153] or by adopting a MOS structure on an undoped GaN layer.[113]

6.6 Epitaxial growth process

Concerning the improvement in device performance as an electron device, a high-purity epitaxial film with low defect density and a high-quality heterointerface having superior flatness and sharpness must be provided, in order to restrain the scattering of carriers as much as possible and to apply a high electric field without breakdown. The active layer of a widegap semiconductor electron device is usually prepared by epitaxial growth, and further development of epitaxial growth technology is indispensable for this purpose. For III–nitride semiconductors, a trial to improve 2DEG characteristics by the insertion of an AlN ultrathin layer at the heterointerface was reported,[154] and our group demonstrated that this method is also effective for the quality improvement of epitaxial layers.[155] On the other hand, we showed that the precise control of the substrate off-angle is critical in obtaining atomically flat surfaces of AlGaN/GaN heteroepitaxial layers appropriate for device processing.[156] Also, for SiC epitaxial growth technology, notable progress has been recently achieved. SiC active layers have been so far
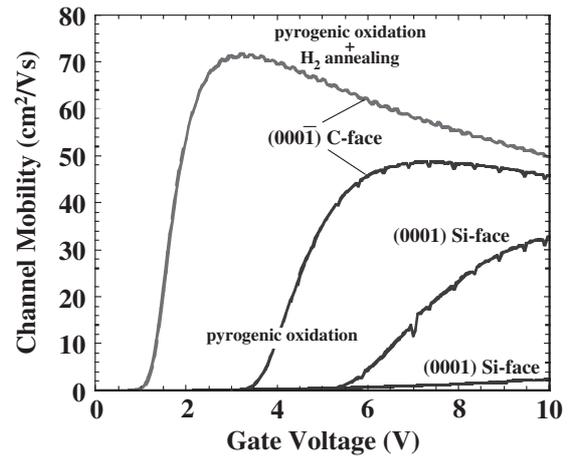
Fig. 19. Crystal face dependence of SiC MOSFET channel mobility. A MOSFET fabricated on a C-face shows markedly higher channel mobility than that on a Si-face. The channel mobility also depends on the formation process of the oxide layer.

grown epitaxially on Si-face off-angle (usually 3.5–8°) (0001) substrates on account of the ease of polytype control.[157] Recently, a technique for epitaxial growth on C-face or small off-angle substrates has been developed,[158,159] and the channel mobility of MOSFETs fabricated on C-face small off-angle (0001) epitaxial wafers was proven to be better by our group.[160] The crystal face dependence of SiC MOSFET channel mobility we obtained is shown in Fig. 19.

To establish device-quality epitaxial wafer technology, the controllability and reproducibility of film thickness, alloy composition, doping concentration and the uniformities of these parameters in a wafer are important. AlGaN/GaN heterostructure wafers with mobilities of 1,000–1,200 cm^2 V^{-1} s^{-1}, and a sheet carrier density of 1×10^{13}/cm^2 (350–500 Ω/□ by sheet resistance) are commercially available; however, many problems remain in uniformity and reproducibility of the quality. If the Al content is 25%, the uniformity within ±5% is almost achieved for 2-in. wafers by current MOCVD epitaxial growth technology; however, the uniformity suddenly deteriorates when Al content exceeds 30%. This is because the uniform transportation of the Al precursor is obstructed by a vapor-phase reaction in an MOCVD furnace. This phenomenon affects the film thickness of AlGaN layers as well as Al content, and it is directly related to the fluctuation in V_{th}. Furthermore, from the viewpoint of device fabrication utilizing existing process facilities, the enlargement of wafer size to 3 or 4 in. is desired; however, it will be necessary to ensure the uniformity and controllability of wafer characteristics in the near future. At that time, the reduction of bending for large-diameter wafers is also required. A composition uniformity of ±1% has been recently reported for AlGaN epitaxial growth on 4-in. substrates with an Al content of 26%.[161] It is necessary to promote such a steady attempt for practical utilization of widegap semiconductor HF devices. The situation is the same for SiC epitaxial wafers, and several excellent results on large-size multiwafer growth have been reported.[162,163]

Figure 20 shows an example of an Al content versus sheet
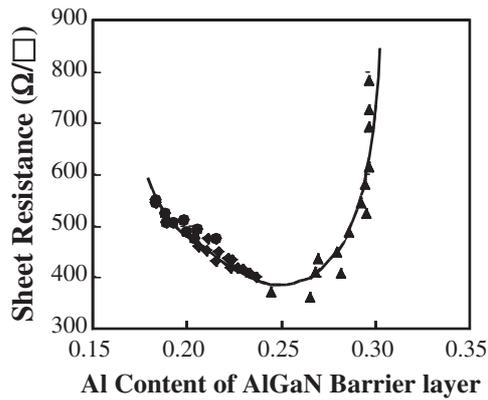
Fig. 20. Example of relationship between Al content and sheet resistance for AlGaN/GaN heterostructure wafer.

resistance relationship obtained from the mapping data of the electrical characteristics of an AlGaN/GaN wafer. There is a clear correlation between the Al content distribution and the 2DEG characteristics. The result shows that the sheet resistance increases because a piezoelectric field is not applied to the AlGaN layer by lattice relaxation, when the Al content exceeds 27% under this growth condition. In terms of epitaxial growth technology for realizing the low sheet resistance profitable to high-power operation, how to raise the Al content up to the point where lattice relaxation takes place is a key point. In addition, an increase in Al content usually deteriorates the surface morphology of HEMT wafers even by the present advanced MOVPE technique, which is highly undesirable for the succeeding device fabrication process. As a technique for growing high-Al-content HEMT wafers without surface deterioration, we proposed the use of a quasi-alloy by adopting a superlattice structure, and demonstrated sheet resistances less than 200 $\Omega/\square$ with an atomically flat surface simultaneously[164] as shown in Fig. 21.

6.7 Substrates

As regards bare substrates for device fabrication, the quality improvement of low-resistance or semi-insulating SiC wafers is a serious issue for both SiC and III–nitride devices. Because an SiC ingot is usually obtained by a sublimation method called the modified Lely method,[165] which is quite different from the Czochralski method for Si,

special care should be taken for the quality improvement of SiC ingots. The reduction in the density of micropipe defects, which seriously deteriorate the V_B of SiC devices, had been the most important problem for a long time for SiC substrates; however, the reduction down to levels equal to or less than 10 and 1 cm^{-2} has now been achieved for 4- and 3-in. substrates, respectively. The solution to this problem has been almost found, together with the size enlargement up to 4 in.

Concerning lateral HF devices, the improvement in DC and HF characteristics is confirmed by the use of semi-insulating substrates.[166–168] The semi-insulating characteristic has been conventionally obtained by V doping;[169] however, the fact that the generated deep levels induce drain current decrease was pointed out, and semi-insulating substrates prepared from high-purity materials and compensated with intrinsic point defects instead of V dopants have become the mainstream.[170] HF output densities higher than 20 W/mm were achieved for AlGaN/GaN HFET using such an SiC substrate of high quality. On the other hand, for vertical high-power switching devices, higher wafer quality with, in particular, a smaller density of device-degrading defects that enables larger current capacity is requested. In addition, the contribution of substrate resistance in the total on-resistance has become nonnegligible after sufficiently reducing on-resistance. Further reduction in substrate specific resistance to levels as low as 10 mΩ cm is much desired, although higher N-doping is more likely to deteriorate the crystalline quality of SiC bulk ingots.[171]

From now on, it seems that the technology development takes approaches that involve the reduction in density of etch pits except micropipes, residual stress and the number of small-angle grain boundaries, and the improvement of surface wrapping technology. The etch pit density, which typically expresses the dislocation density, is several thousand/cm^2–10^4/cm^2 for present commercially available wafers. From this viewpoint, quite an innovative SiC bulk growth technique based on a sublimation method named "repeated a-face method (RAF method)" was reported in 2004,[172] demonstrating an outstanding reduction in the density of crystal defects down to 250 and 75 cm^{-2} for 2-in. and 20 mmϕ wafers, respectively, and the consequent improvement in SiC PiN diode performance. In particular, such an ultrahigh quality substrate with extremely low defect density is the critical factor for realizing large-current-

(a)   (b)
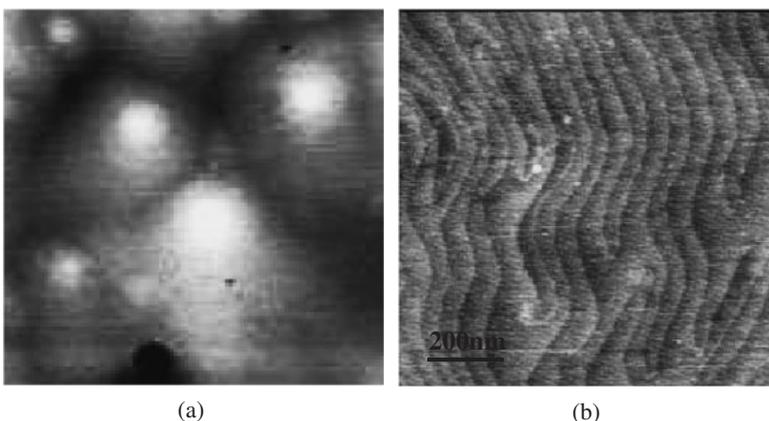
Fig. 21. Atomic force microscope (AFM) surface images for (a) conventional Al$_{0.5}$Ga$_{0.5}$N/GaN and (b) quasi-Al$_{0.5}$Ga$_{0.5}$N/GaN wafers. The quasi-alloy barrier layer of (b) is formed using an AlN/GaN superlattice structure by molecular beam epitaxy (MBE). Although the equivalent Al content is as high as 0.5, the surface of (b) exhibits an atomically flat feature, in contrast to the poor morphology with spiral feature of (a).

density devices that can handle current as high as several tens to a hundred A. On the basis of this result, the confirmation of the equivalent quality is desired at the industrialization level from now on. Other than sublimation-based methods, a solution growth using a metal solvent[173] and a high temperature chemical vapor deposition[174,175] have been newly developed.

As for GaN substrates, bulk crystal growth has been so far tried by the high-pressure preparation,[176] the sublimation method,[177] and the hydride vapor phase epitaxy (HVPE) method.[178] The growth by the flux method using alkali metals has been proposed recently.[179,180] In addition, growth trials by a sublimation method similar to that for SiC have been successively carried out for AlN by several groups,[181–183] and it is necessary to pay attention to the future development of these techniques. For the epitaxial growth of III–nitrides, the use of Si substrates is also available. Si substrates are attractive in terms of large wafer size and cost reduction, although there remain several problems on heat dissipation and HF operation in the millimeterwave region. The quality improvement of epi-layers on Si has been in progress, and quite an excellent quality has been already achieved.[65,112]

6.8 Others

The reduction in FET gate size cannot be avoided for high-frequency and low-loss operation; however, the physical and chemical properties of widegap semiconductors are quite different from Si and GaAs. The development of novel microfabrication technology by, for example, a dry etching technique suitable for widegap semiconductor materials will become important. In particular, new device process technologies such as surface stabilization and selected-area oxidation are necessary for both SiC and III–nitrides.

As for device structure, there are peculiar factors that do not exist in Si and GaAs devices, such as piezoelectric field generattion by stress, anisotropy in a hexagonal structure, and lattice polarity. New approaches different from the conventional one will be necessary for device design. In this sense, processing technology for a p-type layer is also important, even though most of the present widegap semiconductor devices work on the basis of unipolar action. Generally speaking, device-quality p-type layers made of widegap materials are difficult to obtain. However, this is an essential factor for realizing bipolar action devices or junction control in a device structure. Finally, the establishment of the stability and long-term reliability of device performance parameters such as output power, distortion and electrode characteristics is necessary, in order to put high-power devices made of widegap semiconductors to practical use. From these viewpoints, there is a report that III–nitride semiconductor HFET, which is now superior to SiC MESFET in terms of output characteristics, exhibits a two orders of magnitude inferior output stability compared with the latter.[184] On the other hand, attempts to evaluate the device distortion in the context of the implementation to a real amplifier, and to install several switching devices in an inverter module have already begun. It seems that such attempts will be more intensive for the promotion of the practical use of widegap semiconductor power devices in the future.

7. Summary

The characteristics of widegap semiconductors as high-power device materials, and the current status of the development of HF and switching devices using these materials were reviewed. In the research and development of this field, several important breakthroughs have been recently made in crystal growth and device processing, and rapid progress has been achieved in device technology. As a result, a number of device fabrication attempts with high output performances that far surpass those of Si and GaAs devices have been successively reported. It this sense, the superiority of widegap semiconductors has been demonstrated. However, many issues still remain to be solved for realizing practical use, and further progress in research and development is desired. In particular, the importance of device-quality wafer technology including bulk and epitaxial growth should be noted. High-power HF devices and switching devices constitute the key technology that supports wireless communication and power electronics infrastructures, which are the bases of the networks that sustain human society in the 21st century. The development of widegap semiconductor high-power devices should not be delayed in light of their importance.

Acknowledgment

1) S. Yoshida: Parity **11** (1996) 25 [in Japanese].
2) I. Akasaki and H. Amano: Jpn. J. Appl. Phys. **36** (1997) 5393.
3) H. Matsunami: Jpn. J. Appl. Phys. **43** (2004) 6835.
4) H. Ohashi: J. Inst. Electr. Eng. Jpn. **102** (2002) 168 [in Japanese].
5) T. P. Cho: Mater. Sci. Forum **338–342** (2000) 1155.
6) E. O. Johnson: RCA Rev. **26** (1965) 163.
7) R. W. Keyes: Proc. IEEE **60** (1972) 225.
8) B. J. Baliga: J. Appl. Phys. **53** (1982) 1759.
9) B. J. Baliga: IEEE Electron Device Lett. **10** (1989).
10) K. Shenai, R. S. Scott and B. J. Baliga: IEEE Trans. Electron Devices **36** (1989) 1811.
11) P. M. Asbeck, E. T. Yu, S. S. Lau, G. J. Sallivan, J. van Hove and J. Redwing: Electron. Lett. **33** (1997) 1230.
12) O. Ambacher, J. Majeweski, C. Miskys, A. Link, M. Hermann, M. Eickhoff, M. Stutzmann, F. Bernardini, V. Fiorentini, V. Tilak, B. Schaff and L. F. Eastman: J. Phys.: Condens. Matter **14** (2002) 3399.
13) S. Yoshida: Bull. Electrotech. Lab. **62** (1998) 55 [in Japanese].
14) R. J. Trew, J. B. Yan and P. M. Mock: Proc. IEEE **79** (1991) 598.
15) W. Saito, I. Omura, T. Ogura and H. Ohashi: Solid-State Electron. **48** (2004) 1555.
16) D. I. Florescu, V. M. Asnin, F. H. Pollak, A. M. Jones, J. C. Ramer, M. J. Schuman and I. Ferguson: Appl. Phys. Lett. **77** (2000) 1464.
17) A. Jezowski, P. Stachowiak, T. Suski, S. Krukowski, M. Bockowski, J. Grzegory and B. Danilchenko: Phys. Status Solidi B **240** (2003) 447.
18) S. T. Allen, R. A. Sadler, T. S. Alcorn, J. Sumakeris, R. C. Glass, C. H. Carter, Jr. and J. W. Palmour: Mater. Sci. Forum **264–268** (1998) 953.
19) S. Sriram, G. Augustine, A. A. Burk, R. C. Glass, H. M. Hobgood, P. A. Orphanos, L. B. Rowland, T. J. Smith, C. D. Brandt, M. C. Driver

and R. H. Hopkins: IEEE Electron Device Lett. **17** (1996) 369.

20) K. E. Moore, C. E. Weitzel, K. J. Nordquist, L. L. Pond, III, J. W. Palmour, S. Allen and C. H. Carter, Jr.: IEEE Electron Device Lett. **18** (1997) 69.

21) S. T. Allen, T. Alcorn, H. Hagleitner, J. Henning, C. Janke, Z. Ring, S. Sriram, A. Ward and J. Palmour: Final Prog. European Conf. Silicon Carbide and Related Materials 2002, Linköping, 2002, WeIN-01.

22) J. Palmour, S. Allen, S. Sheppard, W. Pribble, R. Sadler, T. Alcorn, W. Ring and C. Carter, Jr.: Conf. Dig. 57th Device Research Conf., Santa Barbara, 1999, p. 38.

23) S. Allen, W. Pribble, R. Sadler, T. Alcon, Z. Ring and J. Palmour: Dig. IEEE MTT-S Int. Microwave Symp., Anaheim, 1999, p. 324.

24) C. E. Weitzel: IEEE Trans. Electron Devices **43** (1990) 1732.

25) A. W. Morse, P. M. Esker, R. C. Clarke, C. D. Brandt, R. R. Siergiej and A. K. Agarwal: Dig. IEEE MTT-S Int. Microwave Symp., San Francisco, 1996, p. 677.

26) A. Morse, P. Esker, S. Sriram, J. Hawkins, I. Chen, J. Ostop, T. Smith, C. Davis, R. Barron, R. Clarke, R. Siergiej and C. Brandt: Dig. IEEE MTT-S Int. Microwave Symp., Denver, 1997, p. 53.

27) S. Sriram, A. Ward, C. Janke, T. Alcorn, H. Hangleitner, J. Henning, K. Wieber, J. Jenny, J. Sumakeris and S. Allen: Mater. Sci. Forum **457–460** (2003) 1205.

28) M. Arai, S. Ono and C. Kimura: Electron. Lett. **40** (2004) 1026.

29) U. K. Mishra, P. Parikh and Y. F. Wu: Proc. IEEE **90** (2002) 1022.

30) L. F. Eastman and U. K. Mishra: IEEE Spectrum **39** (2002) 28.

31) Y. Ohno and M. Kuzuhara: IEEE Trans. Electron Devices **48** (2001) 517.

32) M. A. Khan, J. N. Kuznia, A. R. Bhattarai and D. T. Olsen: Appl. Phys. Lett. **62** (1993) 1786.

33) S. C. Binari, L. B. Rowland, W. Kruppa, G. Kelner, K. Doverspike and D. K. Gaskill: Electron. Lett. **30** (1994) 1248.

34) M. A. Khan, J. M. van Hove, J. N. Kuznia and D. T. Olsen: Appl. Phys. Lett. **58** (1991) 2408.

35) M. A. Khan, J. N. Kuznia, J. M. van Hove, N. Pan and J. Carter: Appl. Phys. Lett. **60** (1992) 3027.

36) M. A. Khan, Q. Chen, C. J. Sun, M. Shur and B. Gelmont: Appl. Phys. Lett. **67** (1995) 1429.

37) J. M. Redwing, M. A. Tischler, J. S. Flynn, S. Elhamri, M. Ahoujja, R. S. Newrock and W. C. Mitchel: Appl. Phys. Lett. **69** (1996) 963.

38) C. F. Lin, H. C. Cheng, J. A. Huang, M. S. Feng, J. D. Duo and G. C. Chi: Appl. Phys. Lett. **70** (1997) 2583.

39) E. Frayssinet, W. Knap, P. Lorenzini, N. Grandjean, J. Massies, C. Skierbiszewski, T. Suski, I. Grzegory, S. Porowski, G. Simin, X. Hu, M. A. Khan, M. S. Shur, R. Gaska and D. Maude: Appl. Phys. Lett. **77** (2000) 2551.

40) M. J. Manfra, L. N. Pfeiffer, K. W. West, H. L. Stormer, K. W. Baldwin, J. W. P. Hsu, D. V. Lang and R. J. Molnar: Appl. Phys. Lett. **77** (2000) 2888.

41) M. A. Khan, A. Bhattarai, J. N. Kuznia and D. T. Olsen: Appl. Phys. Lett. **63** (1993) 1214.

42) M. A. Khan, Q. Chen, M. S. Shur, B. T. Dermott, J. A. Higgins, J. Burm, W. J. Schaff and L. F. Eastman: IEEE Electron Device Lett. **17** (1996) 584.

43) R. Gaska, Q. Chen, J. Yang, A. Osinsky, M. A. Khan and M. S. Shur: IEEE Electron Device Lett. **18** (1997) 492.

44) A. T. Ping, Q. Chen, J. W. Yang, M. A. Khan and I. Adesida: IEEE Electron Device Lett. **19** (1998) 54.

45) G. J. Sullivan, M. Y. Chen, J. A. Higgins, J. W. Yang, Q. Chen, R. L. Pierson and B. T. McDermott: IEEE Electron Device Lett. **19** (1998) 198.

46) J. Mita, H. Okita, K. Kaifu, T. Yamada, Y. Sano, H. Ishikawa, T. Egawa and T. Jimbo: Dig. 61st Device Research Conf., Salt Lake City, 2003, Late News II.A-9.

47) M. Micovic, N. S. Nguyen, P. Janke, W.-S. Wong, P. Hashimoto, L.-M. McCray and C. Nguyen: Electron. Lett. **36** (2000) 358.

48) V. Kumar, W. Lu, R. Schwindt, A. Kuliev, G. Simin, J. Yang, M. A. Khan and I. Adesida: IEEE Electron Device Lett. **23** (2002) 455.

49) M. Higashiwaki and T. Matsui: Jpn. J. Appl. Phys. **44** (2005) L475.

50) T. Inoue, Y. Ando, H. Miyamoto, T. Nakayama, Y. Okamoto, K. Hataya and M. Kuzuhara: IEEE Trans. Microwave Theory Tech. **53** (2005) 74.

51) Y. F. Wu, B. P. Keller, P. Fini, S. Keller, T. J. Jenkins, L. T. Kehias,

52) S. P. DenBaars and U. K. Mishra: IEEE Electron Device Lett. **19** (1998) 50.

52) S. Keller, Y. F. Wu, G. Parish, N. Ziang, J. J. Xu, B. P. Keller, S. P. DenBaars and U. K. Mishra: IEEE Trans. Electron Devices **48** (2001) 552.

53) L. F. Eastman, V. Tilak, V. Kaper, J. Smart, R. Thompson, B. Green, J. R. Shealy and T. Prunty: Phys. Status Solidi A **194** (2002) 433.

54) Y.-F. Wu, A. Saxler, M. Moore, R. P. Smith, S. Sheppard, P. M. Chavarkar, T. Wisleder, U. K. Mishra and P. Parikh: IEEE Electron Device Lett. **25** (2004) 117.

55) C. Lee, H. Wang, J. Yang, L. Witkowski, M. Muir, M. A. Khan and P. Saunier: Electron. Lett. **38** (2002) 924.

56) M. Kuzuhara, H. Miyamoto, Y. Ando, T. Inoue, Y. Okamoto and T. Nakayama: Phys. Status Solidi A **200** (2003) 161.

57) L. F. Eastman: Proc. 28th Int. Symp. Compound Semiconductors, Tokyo, 2001, p. 60.

58) Y. F. Wu, B. P. Keller, S. Keller, J. J. Xu, S. P. DenBaars and U. K. Mishra: IEICE Trans. Electron. **E82-C** (1999) 1895.

59) Y. Ando, Y. Okamoto, H. Miyamoto, N. Hayama, T. Nakayama, K. Kasahara and M. Kuzuhara: IEDM Tech. Dig., 2001, p. 381.

60) Y. F. Wu, D. Kapolnek, J. P. Ibbetson, P. Parikh, B. P. Keller and U. K. Mishra: IEEE Trans. Electron Devices **48** (2001) 586.

61) J. W. Palmour, S. T. Sheppard, R. P. Smith, S. T. Allen, W. L. Pribble, T. J. Smith, Z. Ring, J. J. Sumakeris, A. W. Saxler and J. W. Milligan: IEDM Tech. Dig., 2001, p. 385.

62) S. T. Sheppard, R. P. Smith, W. L. Pribble, Z. Ring, T. Smith, S. T. Allen, J. Milligan and J. W. Palmour: 60th Device Research Conf. Dig., Santa Barbara, 2002, p. 175.

63) Y. Okamoto, Y. Ando, K. Hatara, T. Nakayama, H. Miyamoto, T. Inoue, M. Senda, K. Hirata, M. Kosaki, N. Shibata and M. Kuzuhara: IEEE Trans. Microwave Theory Tech. **52** (2004) 2536.

64) T. Kikkawa, T. Mitani, H. Hayashi, M. Kanamura, S. Yokokawa, M. Nishi, N. Adachi, M. Yokoyama, Y. Tateno and K. Joshin: Dig. IEEE Int. Microwave Symp., Fort Worth, 2004, p. 1347.

65) R. Therrien, S. Singhal, J. W. Johnson, W. Nagy, R. Borges, A. Chaudhari, A. W. Hanson, A. Edwards, J. Marquart, P. Rajagopal, C. Park, I. C. Kizilyalli and K. J. Linthicum: IEDM Tech. Dig., 2005, 23.1.

66) Y.-F. Wu, M. Moore, A. Saxler, T. Wisleder, U. K. Mishra and P. Parikh: IEDM Tech. Dig., 2005, 23.5.

67) H. Kawai, M. Hara, F. Nakamura, T. Asatsuma, T. Kobayashi and S. Imanaga: J. Cryst. Growth **189–190** (1998) 738.

68) N. Maeda, T. Makimura, T. Maruyama, C. Wang, M. Hiroki, H. Yokoyama, T. Makimoto, T. Kobayashi and T. Enoki: Jpn. J. Appl. Phys. **44** (2005) L646.

69) T. Nakayama, Y. Ando, Y. Okamoto, T. Inoue and H. Miyamoto: Electron. Lett. **42** (2006) 489.

70) J. Pankove, S. S. Chang, H. C. Lee, R. J. Molnar, T. D. Moustakas and B. van Zeghbroeck: IEDM Tech. Dig., 1994, p. 389.

71) S. S. Chang, J. Pankove, M. Leksono and B. van Zeghbroeck: 53rd Device Research Conf. Dig., Charlottesfille, 1995, IVB-5.

72) L. S. McCarthy, P. Kozodoy, M. Rodwell, S. DenBaars and U. Mishra: IEEE Electron Device Lett. **20** (1999) 277.

73) B. S. Shelton, J. J. Huang, D. J. H. Lambert, T. G. Zhu, M. M. Wang, C. J. Eiting, H. K. Kwon, M. Feng and R. D. Dupuis: Electron. Lett. **36** (2000) 80.

74) H. Xing, P. Chavarcar, D. S. Green, D. Jena, S. Keller, U. K. Mishra and S. P. DenBaars: Int. Workshop Nitrides Semiconductors Abstr., Aachen, 2002, p. 114.

75) T. Makimoto, K. Kumakura and N. Kobayashi: Appl. Phys. Lett. **79** (2001) 380.

76) T. Makimoto, K. Kumakura and N. Kobayashi: Proc. 5th Int. Conf. Nitride Semiconductors, Nara, 2003, p. 195.

77) T. Palacios, A. Chakraborty, S. Keller, S. P. DenBaars and U. K. Mishra: Dig. 63rd Device Research Conf., Santa Barbara, 2005, p. 181.

78) C. Ota, J. Nishio, T. Hatakeyama, T. Shinohe, K. Kojima, S. Nishizawa and H. Oohashi: Ext. Abstr. (2005 Spring Meet.); Japan Society of Applied Physics, Saitama, 2005, 31a-YK-10 [in Japanese].

79) H. Tsuchida, I. Kamata, T. Miyanagi and T. Nakamura: Ext. Abstr. (2005 Spring Meet.); Japan Society of Applied Physics, Saitama, 2005, 31p-YK-9 [in Japanese].

80) J. H. Zhao, P. Alexandrov and X. Li: IEEE Electron Device Lett. **24**

Jpn. J. Appl. Phys., Vol. 45, No. 10A (2006)

H. OKUMURA

(2003) 402.

81) A. R. Powell, R. T. Leonared, M. F. Brady, St. G. Müller, V. F. Tsvetkov, R. Trussell, J. J. Sumakeris, H. McD. Hobgood, A. A. Burk, R. C. Glass and C. H. Carter, Jr.: Mater. Sci. Forum **457–460** (2004) 41.

82) H. Lendenmann, F. Dahlquist, J. P. Bergman, H. Bleichner and C. Hallin: Mater. Sci. Forum **389–393** (2002) 1259.

83) R. K. Malhan, H. Nakamura, S. Onda, D. Nakamura and K. Hara: Mater. Sci. Forum **433–436** (2003) 917.

84) Y. Tanaka, S. Nishizawa, K. Fukuda, K. Arai, T. Ohno, N. Oyanagi, T. Suzuki and T. Yatsuo: Appl. Phys. Lett. **83** (2003) 377.

85) Y. Sugawara, D. Takayama, K. Asano, R. Singh, J. Palmour and T. Hayashi: Proc. 2001 Int. Symp. Power Semiconductor Devices and ICs, Osaka, 2001, p. 27.

86) M. K. Das, J. J. Sumakeris, B. A. Hull, J. Richmond, S. Krishnaswami and A. R. Powell: Mater. Sci. Forum **483–485** (2005) 965.

87) G. Deboy, M. Marz, J. P. Stengl, H. Strack, J. Tihanyi and H. Weber: IEDM Tech. Dig., 1998, p. 683.

88) http://www.rohm.co.jp/news/1

89) S. H. Ryu, S. Krishnaswami, M. Das, B. Hull, J. Richmond, A. Agarwal, J. Palmour and J. Scoefield: Proc. Int. Symp. Power Semiconductor Devices and ICs, Santa Barbara, 2005, p. 275.

90) S. Harada, M. Okamoto, T. Yatsuo, K. Adachi, K. Fukuda and K. Arai: Proc. Int. Symp. Power Semiconductor Devices and ICs, Kitakyushu, 2004, p. 313.

91) S. Harada, M. Kato, M. Okamoto, T. Yatsuo, K. Fukuda and K. Arai: Proc. Int. Symp. Power Semiconductor Devices and ICs, Naples, 2006, p. 125.

92) J. Tan and J. A. Cooper, Jr.: IEEE Electron Device Lett. **19** (1998) 487.

93) S.-H. Ryu, S. Krishnaswami, M. Das, J. Rchimond, A. Agarwal, J. Palmour and J. Scofield: Mater. Sci. Forum **483–485** (2005) 797.

94) http://www.siced.de/

95) Y. Sugawara, K. Asano, D. Takayama, S. Ryu, R. Singh, J. Palmour and T. Hayashi: Mater. Sci. Forum **389–393** (2002) 1199.

96) Y. Tanaka, K. Yano, M. Okamoto, A. Takatsuka, K. Fukuda, M. Kasuga, K. Arai and T. Yatsuo: Proc. Int. Conf. Silicon Carbide and Related Materials 2005, Pittsburgh, 2005, p. 46.

97) D. Stephani: Abstr. Symp. Future Electron Device 2001, Tokyo, 2001, p. 3.

98) K. Asano, Y. Sugawara, S. Ryu, R. Singh, J. Palmour, T. Hayashi and D. Takayama: Proc. 2001 Int. Symp. Power Semiconductor Devices and ICs, Osaka, 2001, p. 23.

99) Y. Li, P. Alexandrov, J. Zhang, L. X. Li, J. H. Zhao and M. Su: Abstr. Int. Conf. Silicon Carbide and Related Materials 2005, Pittsburgh, 2005, p. 11.

100) J. H. Zhao, K. Tone, P. Alexandrov, L. Fursin and M. Weiner: Proc. Int. Conf. Power Semiconductor Devices and ICs, Cambridge, 2003, p. 50.

101) S. Krishnaswami, A. Agarwal, C. Capell, J. Richmond, S.-H. Ryu, J. Palmour, S. Balachandran, T. P. Chow, S. Bayne, B. Geil, K. A. Jones and C. Scozzie: Mater. Sci. Forum **483–485** (2005) 901.

102) A. Agarwal, S.-H. Ryu, C. Capell, J. Richmond, J. Palmour, H. Bartlow, P. Chow, S. Scozzie, W. Tipton, S. Baynes and K. Jones: Mater. Sci. Forum **457–460** (2004) 1141.

103) J. H. Zhao, J. Zhang, P. Alexandrov, X. Li and T. Burke: Mater. Sci. Forum **457–460** (2004) 1173.

104) Y. Sugawara, D. Takayama, K. Asano, A. Agarwal, S. Ryu, J. Palmour and S. Ogata: Proc. Int. Symp. Power Semiconductor Devices and ICs, Kitakyushu, 2004, p. 365.

105) N.-Q. Zhang, B. Moran, S. P. DenBaars, U. K. Mishra, X. W. Wang and T. P. Ma: Phys. Status Solidi A **188** (2001) 213.

106) S. Yoshida and H. Ishii: Phys. Status Solidi A **188** (2001) 243.

107) W. Saito, Y. Takada, M. Kuraguchi, K. Tsuda, I. Omura and T. Ogura: IEDM Tech. Dig., 2003, p. 587.

108) N.-Q. Zhang, B. Moran, S. P. DenBaars, U. K. Mishra, X. W. Wang and T. P. Ma: IEDM Tech. Dig., 2001, p. 589.

109) S. Yagi, M. Shimizu, M. Inada, Y. Yamamoto, G. Piao, H. Okumura, Y. Yano, N. Akutsu and H. Ohashi: Solid-State Electron. **50** (2006) 1057.

110) M. Inada, S. Yagi, Y. Yamamoto, G. Piao, M. Shimizu, H. Okumura, K. Arai, Y. Yano and N. Akutsu: Proc. Int. Symp. Power Semi-conductor Devices and ICs, Naples, 2006, p. 121.

111) S. Yoshida, D. Wang and M. Ichikawa: Jpn. J. Appl. Phys. **41** (2002) L820.

112) M. Hikita, M. Yanagihara, K. Nakazawa, H. Ueno, Y. Hirose, T. Ueda, Y. Uemoto, T. Tanaka, D. Ueda and T. Egawa: IEDM Tech. Dig., 2004, p. 803.

113) K. Matocha, T. P. Chow and R. J. Gutmann: IEEE Trans. Electron Devices **52** (2005) 6.

114) T. Kachi, N. Soejima, T. Uesugi, H. Ueda, M. Kodama, M. Kanechika and M. Sugimoto: Abstr. 6th Int. Conf. Nitride Semi-conductors, Bremen, 2005, Th-P-139.

115) C. Weitzel, L. Pond, K. Moore and M. Bhatnagar: Mater. Sci. Forum **264–268** (1998) 969.

116) D. Qiao, L. S. Yu, S. S. Lau, J. M. Redwing, J. Y. Lin and H. X. Jiang: J. Appl. Phys. **87** (2000) 801.

117) E. J. Miller, X. A. Dang and E. T. Yu: J. Appl. Phys. **88** (2000) 5951.

118) J. H. Mazur, M. Benamara, Z. Liliental-Weber, W. Swider, J. Washburn, C. J. Eiting and R. D. Dupuis: MRS Internet J. Nitride Semicond. **5S1** (2000) W3.77.

119) H. Hasegawa and S. Oyama: J. Vac. Sci. Technol. B **20** (2002) 1647.

120) J. Kotani, T. Hashizume and H. Hasegawa: J. Vac. Sci. Technol. B **22** (2004) 2179.

121) T. Hashizume and H. Hasegawa: Appl. Surf. Sci. **234** (2004) 387.

122) J. W. P. Hsu, M. J. Manfra, R. J. Molnar, B. Heying and J. S. Speck: Appl. Phys. Lett. **81** (2002) 79.

123) B. S. Simpkins, E. T. Yu, P. Walltereit and J. S. Speck: J. Appl. Phys. **94** (2003) 1448.

124) J. E. Northrup: Phys. Rev. B **66** (2002) 045204.

125) K. Shiojima and T. Suemitsu: J. Vac. Sci. Technol. B **21** (2003) 698.

126) D.-H. Cho, M. Shimizu, T. Ide, H. Okita and H. Okumura: Jpn. J. Appl. Phys. **41** (2002) 4481.

127) T. Hashizume, S. Ootomo, T. Inagaki and H. Hasegawa: J. Vac. Sci. Technol. B **21** (2003) 1828.

128) T. Hashizume, S. Ootomo and S. Kishimoto: Appl. Phys. Lett. **83** (2003) 2952.

129) M. Ochiai, M. Akita, Y. Ohno, S. Kishimoto, K. Maezawa and T. Mizutani: Jpn. J. Appl. Phys. **42** (2003) 2278.

130) C. S. Oh, C. J. Youn, G. M. Yang, K. Y. Lim and J. W. Yang: Appl. Phys. Lett. **85** (2004) 4214.

131) Y. Ohno, T. Nakano, S. Kishimoto, K. Maezawa and T. Mizutani: Appl. Phys. Lett. **84** (2004) 2184.

132) Y. Ando, Y. Okamoto, H. Miyamoto, T. Nakayama, T. Inoue and M. Kuzuhara: IEEE Electron Device Lett. **24** (2003) 289.

133) Y. Wu, M. Moore, T. Wisleder, P. M. Chavarkar, U. K. Mishra and P. Parikh: IEDM Tech. Dig., 2004, p. 1078.

134) Y. Ando, A. Wakejima, Y. Okamoto, T. Nakayama, K. Ota, K. Yamanoguchi, Y. Murase, K. Kasahara, K. Matsunaga, T. Inoue and H. Miyamoto: IEDM Tech. Dig., 2005, 23.3.

135) S. C. Binari, W. Kruppa, H. B. Dietrich, G. Kelner, A. E. Wickenden and J. A. Freitas, Jr.: Solid-State Electron. **41** (1997) 1549.

136) R. Vetury, N. O. Zhang, S. Keller and U. K. Mishra: IEEE Trans. Electron Devices **48** (2001) 560.

137) T. Mizutani, Y. Ohno, M. Akita, S. Kishimoto and K. Maezawa: Phys. Status Solidi A **194** (2002) 447.

138) H. Hasegawa, T. Inagaki, S. Ootomo and T. Hashizume: J. Vac. Sci. Technol. B **21** (2003) 1844.

139) O. Noblanc, C. Arnodo, C. Dua, E. Chartier and C. Brylinski: Mater. Sci. Forum **338–342** (2000) 1247.

140) K. Hilton, M. Uren, D. Hayes, P. Wilding, H. Johnson, J. Guest and B. Smith: Mater. Sci. Forum **338–342** (2000) 1251.

141) A. K. Agarwal, J. B. Casady, L. B. Rowland, W. F. Valek, M. H. White and C. D. Brandt: IEEE Electron Device Lett. **18** (1997) 586.

142) V. V. Afanas'ev, F. Ciobanu, D. Dimitrijev, G. Pensl and A. Stesmans: Mater. Sci. Forum **563–568** (2005) 483.

143) L. A. Lipkin and J. W. Palmour: J. Electron. Mater. **25** (1996) 909.

144) K. Ueno, R. Asai and T. Tsuji: IEEE Electron Device Lett. **19** (1998) 244.

145) H. F. Li, S. Dimitrijev, H. B. Harrison and D. Sweatman: Appl. Phys. Lett. **70** (1997) 2028.

146) G. Y. Chung, C. C. Tin, J. R. Williams, K. McDonald, R. K. Chanana, R. A. Weller, S. T. Pantelides, L. C. Feldman, O. W. Holland, M. K. Das and J. W. Palmour: IEEE Electron Device Lett. **22** (2001) 176.

147) L. A. Lipkin, M. K. Das and J. W. Palmour: Mater. Sci. Forum **389–393** (2002) 985.

148) H. Yano, T. Hirao, T. Kimoto, H. Matsunami, K. Asano and Y. Sugawara: IEEE Electron Device Lett. **20** (1999) 611.

149) S. Harada, S. Suzuki, J. Senzaki, R. Kosugi, K. Adachi, K. Fukuda and K. Arai: IEEE Electron Device Lett. **22** (2001) 272.

150) J. Senzaki, K. Kojima, T. Suzuki and K. Fukuda: Mater. Sci. Forum **433–436** (2003) 613.

151) J. Senzaki, K. Kojima, T. Kato, J. Shimozato and K. Fukuda: Appl. Phys. Lett. **89** (2006) 022909.

152) S. Jia, Y. Cai, D. Wang, Z. Zhang, K. J. Chen and K. M. Lau: Abstr. 6th Int. Conf. Nitride Semiconductors, Bremen, 2005, Th-P-013.

153) O. Katz, D. Mistele, B. Meyler, G. Bahir and J. Salzman: IEEE Trans. Electron Devices **52** (2005) 146.

154) L. Shen, S. Heikman, B. Moran, R. Corrie, N.-Q. Zhang, D. Buttari, I. P. Smorchkova, S. Keller, S. P. DenBaars and U. Mishra: IEEE Electron Device Lett. **22** (2001) 457.

155) T. Ide, M. Shimizu, S. Hara, D.-H. Cho, K. Jeganathan, X.-Q. Shen, H. Okumura and T. Nemoto: Jpn. J. Appl. Phys. **41** (2002) 5563.

156) X. Q. Shen, M. Shimizu and H. Okumura: Jpn. J. Appl. Phys. **42** (2003) L1293.

157) N. Kuroda, K. Shibahara, W. S. Yoo, S. Nishino and H. Matsunami: Ext. Abstr. 19th Solid State Devices and Materials, Tokyo, 1987, p. 227.

158) S. Nakamura, T. Kimoto and H. Matsunami: J. Cryst. Growth **256** (2003) 341.

159) K. Kojima, H. Okumura, S. Kuroda and K. Arai: J. Cryst. Growth **269** (2004) 367.

160) K. Fukuda, M. Kato, K. Kojima and J. Senzaki: Appl. Phys. Lett. **84** (2004) 2088.

161) M. Miyoshi, H. Ishikawa, T. Egawa and T. Jimbo: Phys. Status Solidi C **0** (2003) 2091.

162) B. Thomas and C. Hecht: Tech. Prog. Int. Conf. Silicon Carbide and Related Materials 2005, Pittsburgh, 2005, p. 30.

163) A. Burk. M. J. O'Loughlin, M. Paisley, A. Powell, M. Brady, R. Leonard and D. McClure: Tech. Prog. Int. Conf. Silicon Carbide and Related Materials 2005, Pittsburgh, 2005, p. 30.

164) Y. Kawakami, X. Q. Shen, G. Piao, M. Shimizu, H. Nakanishi and H. Okumura: 1st Int. Symp. Growth of III–Nitrides, Linköping, 2005, WeP-18.

165) Yu. M. Tairov and V. F. Tsvetkov: J. Cryst. Growth **43** (1978) 209.

166) A. Ellison, B. Magnusson, C. Hemmingsson, W. Magnusson, T. Iakimov, I. Strasta, A. Henry, N. B. Henelius and E. Janzén: Mater. Res. Soc. Symp. Proc. **640** (2001) H-12-1.

167) S. Sriram, G. Augustine, A. Burk, R. Glass, H. Hobgood, P. Orphanos, L. Rowland, T. Smith, C. Brandt, M. Driver and R. Hopkins: IEEE Electron Device Lett. **17** (1996) 369.

168) N. Sghaier, J. M. Bluet, A. Souifi, G. Guillot, E. Morvan and C. Brylinski: Mater. Sci. Forum **389–393** (2001) 1363.

169) H. McD. Hobgood, R. C. Glass, G. Augustine, R. H. Hopkins, J. Jenny, M. Skowronski, W. C. Michel and M. Roth: Appl. Phys. Lett. **66** (1995) 1364.

170) E. Morvan, A. Kerlain, C. Cua and C. Brylinski: Mater. Sci. Forum **433–436** (2003) 731.

171) J. Q. Liu, H. J. Chung, T. Kuhr, Q. Li and M. Skowronski: Appl.

172) D. Nakamura, I. Gunjishima, S. Yamaguchi, T. Ito, A. Okamoto, H. Kondo, S. Onda and K. Takatori: Nature **430** (2004) 1009.

173) K. Kusunoki, S. Munetoh, K. Kamei, M. Hasebe, T. Ujihara and K. Nakajima: Mater. Sci. Forum **457–460** (2004) 123.

174) O. Kordina, C. Hallin, A. Ellison, A. S. Bakin, L. G. Ivanov, A. Henry, R. Yakimova, M. Tuominen, A. Vehanen and E. Janzén: Appl. Phys. Lett. **69** (1996) 1456.

175) A. Ellison, B. Magnusson, B. Sundqvist, G. Pozina, J. P. Bergman and E. Janzén: Mater. Sci. Forum **457–460** (2004) 9.

176) I. Grzegory, J. Jun, M. Bockowski, St. Krukowski, M. Wroblewski, B. Lucznik and S. Porowski: J. Phys. Chem. Solids **56** (1995) 639.

177) S. Kurai, Y. Naoi, T. Abe, S. Ohmi and S. Sakai: Jpn. J. Appl. Phys. **35** (1996) L77.

178) R. J. Molnar, P. Maki, R. Aggarwal, Z. L. Liau, E. R. Brown, I. Melngailis, W. Götz, L. T. Romano and N. M. Johnson: Mater. Res. Soc. Symp. Proc. **423** (1996) 221.

179) F. Kawamura, M. Morishita, T. Iwahashi, M. Yoshimura, Y. Mori and T. Sasaki: Jpn. J. Appl. Phys. **41** (2002) L1440.

180) F. Kawamura, M. Morishita, K. Omae, M. Yoshimura, Y. Mori and T. Sasaki: Jpn. J. Appl. Phys. **42** (2003) L879.

181) M. Bickermann, B. M. Epelbaum and A. Winnacker: Phys. Status Solidi C **0** (2003) 1993.

182) L. J. Schowalter, W. Liu, S. B. Schujman, J. Grandusky, F. Shahedipour-Sandvik, M. Goorskky and M. Wood: Abstr. 6th Int. Conf. Nitrides Semiconductors, Bremen, 2005, Tu-G4-3.

183) V. Soukhoveev, O. Kovalenkov, V. Ivantsov, A. Usikov and V. Dmitriev: Abstr. 6th Int. Conf. Nitrides Semiconductors, Bremen, 2005, Tu-G3-6.

184) S. T. Allen, T. Alcorn, H. Hagleitner, J. Henning, C. Janke, Z. Ring, S. Sriram, A. Ward and J. Palmour: European Conf. Silicon Carbide and Related Materials 2002 Final Program, Linköping, 2002, WeIN-01.

Hajime Okumura studied Chemistry and received his B.E. and M.E. degrees from Kyoto University in 1979 and 1981, respectively. From 1981 to 2000, he served at Electrotechnical Laboratory, Ministry of International Trade and Industry (MITI), as a (senior) researcher. In 1990, he received his Ph. D. degree from Osaka University for the studies of semiconductor heterostructures. He was a guest researcher at the University of Grenoble I under the French government scholarship in 1991, and dispatched to the R&D Association of Future Electron Devices as a general manager for the management of MITI national Projects from 2000 to 2001. He joined Power Electronics Research Center, National Institute of Advanced Industrial Science and Technology (AIST) as a team leader in 2001 when AIST was newly established. Now, he is the Deputy Director of the same research center. His specialty is material science, especially compound semiconductors and their device application. His current research interests are crystal growth, characterization, device processing and their power electronics application concerning widegap semiconductors such as GaN and SiC.